Mirror Symmetry is Subject to Crowding Across the Visual Field

Gabrielle Roddy

A Thesis

In

The Department

Of

Psychology

Presented in Partial Fulfilment of the Requirements

For the Degree of Magistrate in Arts at

Concordia University

Montréal Québec, Canada

July 2011

CONCORDIA UNIVERSITY

School of Graduate Studies

This is to certify that the thesis prepared

By: **Gabrielle Roddy**

Entitled: **Mirror Symmetry is Subject to Crowding Across the Visual Field**

and submitted in partial fulfillment of the requirements for the degree of

Master of Arts (Psychology)

complies with the regulations of the University and meets the accepted standards with respect to originality and quality.

Signed by the final examining committee:

Wayne Brake	Chair
Aaron Johnson	Examiner
Norman Segalowitz	Examiner
Rick Gurnsey	Supervisor

Approved by: Wayne Brake

Chair of Department or Graduate Program Director

Dean of Faculty: Brain Lewis

August 26’2011

ABSTRACT

Mirror Symmetry is Subject to Crowding Across the Visual Field

Gabrielle Roddy

Bilateral mirror symmetry is often thought to be particularly salient to human observers. It has been hypothesized that symmetry engages specialized mechanisms that evolved to sense symmetrical objects in nature. However, although symmetry is a commonly encountered stimulus property, studies have shown that sensitivity to mirror symmetry does not serve an alerting function when embedded in noise (Gurnsey et al., *Can Soc Brain Behav Cog Sci*, 1998b). Further, sensitivity to symmetry decreases similarly to other common stimuli when targets are presented away from the centre of the visual field (for review: Wagemans, *Spat Vis*, 1995).

The three experiments presented in this thesis show that symmetrical targets are vulnerable to the same interference as other stimuli when surrounded by non-target elements. The data shares many of the common characteristics attributable to the crowding phenomenon in current and historical literature (for review: Whitney & Levi, *Trends Cog Sci*, 2011). Namely, we find little or no effect of crowding at fixation. The magnitude of the crowding effect increased nonlinearly with eccentricity and at a greater rate than the linear increase of resolution loss (e.g., Gurnsey et al., *JoV*, 2011; Latham & Whitaker, *Ophthalmic Physiol Opt*, 1996). In this case, standard double linear size scaling procedures were unable to characterize the data across the visual field and produced untenable results that violate assumptions of the crowding phenomenon. Taken together, the results provide evidence that symmetry is unlikely to be processed in parallel fashion by low-level mechanisms.

Acknowledgements

First and foremost I would like to thank my supervisor Dr. Rick Gurnsey for his unflagging support, patience and understanding throughout this process. What I have learned from him is immeasurable. Thank you to Dr. Aaron Johnson and Dr. Micheal von Grunau for always keeping their doors open and helping me through this process. I would like to thank all of my participants and fellow lab members especially Wael Chanab and Bruno Richards, without whom I may have lost my head. Thank you to NSERC, FQRNT and Concordia University for supporting my graduate education thus far and providing me with this opportunity. Finally, to all my friends and family and to Jordy, thank you for listening, through it all.

This research was supported by an NSERC grant awarded to Rick Gurnsey and a CIHR grant awarded to Rick Gurnsey, Aaron Johnson and Micheal von Grunau.

Table of Contents

List of Figures

List of Tables

Introduction

A normally functioning visual system is presented with a continuous stream of information in the course of a single day. The efficiency with which it can process many properties in parallel (simultaneously) is a widely studied topic in vision research (e.g., Gurnsey, Herbert, & Kenemy, 1998b; Treisman & Gelade, 1980, and many others). Many researchers wish to know what stimulus properties might be encoded within the lower level processing mechanisms of the visual system such as those that have been proposed for colour detection (Tresiman & Gelade, 1980). Vertically oriented bilateral symmetry has proved to be extremely salient in some lab settings, which might suggest that it engages specialized mechanisms in the early visual system that have evolved to sense and select symmetrical objects in nature for further processing (Barlow & Reeves, 1979; Locher & Wagemans, 1993). Evidence from the animal kingdom has shown that female finches spend more time displaying courtship behaviour in front of males wearing symmetrically placed leg rings versus those wearing asymmetrical leg rings (Swaddle & Cuthill, 1993). Another well-known study showed that honeybees are able to learn preference for a bilaterally symmetrical signal with a vertical axis over the same pattern rotated by 90º (Horridge, 1996). Results such as these seem to support the notion of a symmetry detecting mechanism. However, symmetry in many forms is ubiquitous in our surroundings and it would serve no useful purpose for the visual system to be constantly alerted to unnecessary visual information. In fact, in the aforementioned study by Horridge (1996) it was quite clear that the bees showed no innate preference for the vertically symmetrical signal until they were trained to do so. As a simple example of the

inconvenience of a visual system alerted to all symmetrical signals encountered in the course of a day, consider navigating through a densely forested area, all the while being alerted to the symmetrical patterns on the leaves of the very trees blocking the way.

Visual stimuli are rarely presented in isolation and it is important for the visual system to be able to locate a specific object, such as a pencil on a crowded desk, when it is surrounded (flanked) by other stimuli, both similar and dissimilar, in a given scene. If specialized mechanisms have evolved to sense symmetrical objects it makes sense to ask whether that mechanism is vulnerable to interference from competing stimuli that surround the target. Before such an examination can be undertaken it is important to understand the large literature on symmetry detection across the visual field. It is also important to understand the limitations of the peripheral visual field to further our understanding and add to our measurements of how the sensitivity to certain physical stimuli might change across the visual field.

Symmetry Detection at Fixation

Whether it is the centre of a form or part of a crowded scene, symmetry is prevalent in architecture, art (especially religious and mystical artworks), utilitarian design, the structure of flowers, and even man-made decorative arrangements of them (Hodgson, 2011; Moriyama & Moriyama, 1999; Van der Helm, 2011). The structural symmetry of many biological forms is frequently hypothesized to underlie our putative sensitivity to visual symmetry. A stimulus pattern is said to be symmetrical when the pattern is mirrored, translated or rotated in any direction in the same plane. The defining character is that any two points of a stimulus remain the same distance apart under such transformations. In other words, “symmetry means self-similarity under a class of

transformations" (Wagemans, 1995, p. 10). However, bilateral mirror symmetry (i.e., a butterfly or heart) has been shown to be the most salient symmetrical pattern in studies of symmetry detection and is therefore most often used in psychophysical research (for review: Wagemans, 1995).

The visual system is thought to use abrupt discontinuities in luminance, orientation, chromaticity, motion or texture to segment aspects of a stimulus prior to identification. These types of local contrasts are thought to be processed in parallel, corresponding all retinal locations, by low-level visual mechanisms. Bilateral symmetry may also offer a local contrast of this type that distinguishes it from cluttered, non-symmetrical surroundings (Gurnsey, Herbert, & Kenemy, 1998a). However, there are factors that would limit the usefulness of a specialized low-level symmetry-selective mechanism. Firstly, forms that are structurally bilaterally symmetrical most often project to the retinas as either skewed symmetries or simply non-symmetrical forms, rather than perfect bilateral symmetry (Wagemans, 1993). In part this is because animate objects rarely position their limbs to produce perfect, object-centred symmetry, and in part because even perfectly symmetrical objects (animate or inanimate) are rarely presented at an angle perpendicular to the line of sight. Secondly, there is a great deal of symmetrical information present in our surroundings and much of it is unnecessary information for the majority of time, consider the previously mentioned symmetry of leaf patterns as an example.

Many studies have looked at sensitivity to a symmetrical target briefly presented at the centre of our gaze (also known as fixation). It has become clear the local pattern information that is most salient to the observer is restricted to a small area surrounding

the axis of symmetry (Barlow & Reeves, 1979; Jenkins, 1982, 1983), especially when the axis of symmetry is vertical (Barlow & Reeves, 1979; Jenkins, 1985), and presented to the fovea (the area of the eye that is engaged when we are fixating directly on a target) (Barlow & Reeves, 1979; Saarinen, 1988).

Barlow and Reeves (1979) asked participants to indicate from which of two populations (symmetrical vs. non symmetrical) a foveally presented pattern comprising 100 dots was drawn. The patterns differed in their proportion of symmetric versus random dots. Barlow and Reeves found that sensitivity to symmetry increased as the number of symmetrical dot pairs within the pattern increased. When the paired dots were close to the vertical axis observers were most efficient when discriminating between a random pattern and a symmetrical one. Sensitivity was also high when the dots paired across the vertical midline were at the outer edges of the stimulus. Sensitivity to the symmetrical pattern was lowest when dot pairs were at an intermediate distance between the axis and the edge.

There also seemed to be a hierarchical pattern of the sensitivity to the axis of symmetry orientation in that participants were most sensitive to vertical axes of symmetry, followed by horizontal axes and then the oblique axes (i.e., ± 45º). The vertical axis bias has been replicated by other researchers (e.g., Wagemans, 1992; Wenderoth, 1994). However, a few studies have produced different hierarchies of sensitivity (Jenkins, 1983; 1985). It should also be noted that Wenderoth (1994) showed that by manipulating the range of orientations in any one block of trials the vertical bias could be reversed or changed. (We will return to this point in the General Discussion.)

Barlow and Reeves (1979) sought to determine the degree of precision the perceptual system might demand of paired dots when they are jittered across the vertical midline. The greatest reduction of sensitivity occurred when the dots were jittered near the vertical axis and the percent of correct responses could be reduced to chance if the jittered strip exceeded approximately ±1.2º in displays comprising 100 hundred dots each. Tyler, Hardage and Miller (1995) found that the visual system could tolerate a loss of information of up to 3º across the vertical midline of a symmetrical target, although their stimulus was much larger than that of Barlow and Reeves (1979). Tyler et al. used a static dot display comprising 307,200 dots coloured either randomly black and white over the entire screen or for the symmetrical stimuli, mirrored around a gap of a given width at the midline which was filled with randomly coloured dots (the dots subtended 2.2 arcmin when viewed at 57 cm and filled a 23.5 wide by 17.6º high screen (pixel resolution was set at 640 horizontal by 480 vertical).

The studies discussed so far have dealt with symmetry perception when targets are presented at or near the fovea. However, it is well documented that visual sensitivity to targets of fixed size changes across the visual field due to limitations at both the retinal and cortical levels (e.g., Gurnsey, Roddy, Ouhnana, & Troje, 2008; Levi, Klein, & Aitsebaomo, 1985; Rovamo & Virsu, 1979; Weymouth, 1958). It is therefore necessary to look at how perceptual sensitivity might change when symmetrical targets are presented further into the peripheral visual field.

The Peripheral Visual Field

There are inherent perceptual limitations that can greatly affect the perception of fine pattern details as stimuli are moved from the fovea into the peripheral region. (Note:

distance from the fovea is known as eccentricity and is measured in degrees of visual angle.) The following paragraphs outline the factors involved in the limited resolution of the peripheral visual field that occur at both the retinal and cortical level.

In the retina, the transduction (conversion) of photons (the basic unit of light) to electrical signals is performed by rod and cone receptors. The fovea is composed entirely of cone receptors, which provide high acuity for resolving spatial detail, colour and spatial arrangements. When we are fixating on an object, light waves reflect from objects to the back of the eye where they are absorbed by the cone receptors. Studies on the macaque monkey show that up to approximately 10º eccentricity the cones converge onto the ganglion cell receptors at a ratio of about 1:1 (Wilson, Levi, Maffei, Rovamo & Devalois, 1990). However, after 10º the cones become larger, spaced farther apart and the cone-to-ganglion-cell ratios begin to decrease with increasing eccentricity converging on a ratio of about 1:2 (Perry & Cowey, 1985; Wilson et al., 1990). This causes what is known as visual under-sampling, or resolution loss.

Thibos, Cheney and Walsh (1987) suggested that the pattern resolution capabilities of the peripheral retinal regions are only partly limited by the increasing cone-to-ganglion-cell convergence ratios. The increase in cone receptor size also limits pattern resolution, because although the larger surface of the peripheral receptors can catch more photons the information is diffused (Thibos, Cheney, & Walsh, 1987). This leads to uncertainty about the location at which the photon struck the retina and therefore decreases the acuity of the image.

There are cortical constraints on peripheral visual acuity as well as the aforementioned retinal limitations. Once the light has been transduced at the retinal level

the electrical signals travel via bipolar cells to relay cells in the thalamus, a sensory relay station situated between the cerebral cortex and midbrain (a portion of the central nervous system near the centre of the brain). Within the thalamus a structure known as the lateral geniculate nucleus (LGN) serves as the primary relay mechanism of visual information to the primary visual cortex, (especially layer IV of the striate cortex) known as area V1.

In the LGN there is further convergence as there are two to three LGN relay cells per ganglion cell axon for the foveal representation and that number drops to only about one per two ganglion cell axons across the periphery (Connolly & Van Essen, 1984). Put differently, it is estimated that there are approximately 1000 striate cells per incoming LGN axon originating from the fovea but that number drops to only 100 for peripheral information (Dow, Snyder, Vautin, & Bauer, 1981). Therefore, the number of cones connected to a $1mm^2$ region of cortex, for example, also decreases with eccentricity and the representation from the central 5º of the visual field comes to occupy over 40º of the striate cortex (Wilson et al., 1990). This overrepresentation is known as the cortical magnification factor (CMF) and it has been well established in animal research (Connolly & Van Essen, 1984; Daniel & Whitteridge, 1961; Dow et al., 1981; Hubel & Weisel, 1974).

The studies of Daniel and Whitteridge (1961) on the striate cortex of the macaque monkey have been especially influential with respect to estimations of the CMF. They measured the angular distance separating the centres of two receptive fields in the visual field and the linear distance between the corresponding points on the cortical surface. They coined the term 'linear magnification' factor to refer to the number of millimetres of cortex representing one degree of visual angle at a given eccentricity. One degree of

visual angle at the fovea represents about 6 to 8 mm linearly on the surface of the cortex. From these measures, Daniel and Whitteridge (1961) noted a systematic linear decline in the CMF with increasing eccentricity (up to 60º).

In their seminal studies on the visual systems of cats, Hubel and Wiesel (1974) found that receptive field size and cortical magnification vary similarly with increasing eccentricity from 1 to 20º. They also noted that the product of cortical magnification and receptive field size, about 1 mm, was more or less constant regardless of visual field location. The constancy of the pattern and the fact that 1 mm is the size of a hypercolumn (a cortical column within which all orientations are represented) suggested there might be uniformity in the structure of the cortex.

From the animal literature just reviewed it is clear that spatial sampling from the retina to the striate cortex converges with eccentricity. The rate at which it occurs is limited by the anatomical constraints of cone density decreases and ganglion cell convergence, and/or the cortical constraints of the CMF. It is of great interest to vision scientists to measure psychophysical performance in human observers in a variety of perceptual tasks and relate changes in performance across the visual field to the suggested representation of the anatomical map.

M-Scaling

As previously mentioned, sensitivity to spatial structure decreases quickly as stimuli are moved from the foveal region to the periphery of the visual field. Rovamo and Virsu (1979) proposed that the cortical limitations of the peripheral visual field could be overcome by magnifying stimuli, at a given position in the visual field, in all dimensions using scaling factors based on the CMF estimates from animal studies (e.g., Cowey &

Rolls 1974; Dow et al., 1981). These estimates were believed to correspond to decreasing ganglion cell density with increasing eccentricity. This procedure is known as *M*-scaling (Rovamo and Virsu, 1979). *M*-scaling has as its base the assumption that the decline in visual performance with eccentricity is related proportionally to anatomical and physiological changes across the visual system (Cowey & Rolls, 1974; Weymouth, 1958). To derive formulas to calculate psychophysical estimates of the CMF, Rovamo and Virsu (1979) first divided the visual field into four principal half meridians. The formulas were intended to characterize change in receptive field density as a function of eccentricity and allow predictions of visual acuity in various psychophysical tasks. Using previous estimates of ganglion cell density in humans as estimated by Drasdo (1977; as cited in Rovamo and Virsu, 1979, p. 498) Rovamo and Virsu (1979) developed four formulas. The following is their equation for the Superior visual field:

$$M_s = (1 + .42E + 0.00012E^3)^{-1} M_0, \ (0 \le E \le 45^\circ) \qquad (1a)$$

where M_s represents the factor by which the processing area for a stimulus of fixed size presented foveally decreases with the CMF as the stimulus is moved farther into the periphery. (Note: In this case a 1º stimulus presented foveally represents approximately 8 mm (M_0) of striate cortex.)

If we simplify Equation 1a by dropping the cubic factor ($.000112\ E^3$) we find that

$$M_s = 1/(1 + .42E)M_0 \qquad (1b)$$

thus

$$M_s = M_0/(1 + .42E) \qquad (1c).$$

Therefore to determine the rate of magnification (F) at eccentricity (E) to compensate for acuity loss due decreased ganglion cell density (as characterized by M_s) we calculate F as follows:

$$F = 1 + .42E$$

$$\text{or more generally } F = 1 + KE \tag{2a}$$

where K = .42. When F = 2 (to represent that point at which stimuli need to be doubled to achieve the foveal standard), then,

$$2 = 1 + KE \tag{2b}$$

therefore,

$$2 = 1 + .42E \tag{2c}$$

and

$$1 = .42E \tag{2d}$$

which is simplified to

$$1 / .42 = E \tag{2e}.$$

Because E is the eccentricity at which stimulus size must double (e.g., F = 2) to overcome peripheral under-sampling, we refer to it as E_2. Therefore, the rate at which stimuli must be magnified relative to the foveal standard to compensate for ganglion cell convergence in a human is given by $F = 1 + E / E_2$; in this case, $E_2 = 1 / .42 = 2.38$. For simplicity, the results section of this thesis will be presented using the parameter k to reflect the *rate* of magnification required to collapse eccentric data to the foveal data therefore smaller numbers refer to slower sensitivity loss and, as the values increase, so too does the rate of magnification.

Although *M*-scaling stimuli in the periphery with preset scaling factors representing the decrease in receptive field density proved useful for tasks such as Snellen Acuity (the letter chart used during an eye exam) and grating detection (Virsu, Näsänen & Osomoviita, 1987), it failed in many tasks that require precise encoding of spatial relationships. (Saarinen, 1988; Saarinen, Rovamo, & Virsu, 1989; Virsu et al., 1987). For example, Levi, Klein and Aitsebaomo (1985) conducted a series of psychophysical experiments on vernier acuity (i.e., the ability to discriminate the offset between parallel and abutting lines). Either two abutting rows of seven vertical lines or a simple two-line stimulus was presented out to 10º eccentricity in the lower visual field. When stimuli were scaled with an E_2 value of .77, based on estimates for tasks of spatial positioning from Dow, Snyder, Vautin and Bauer (1981), discrimination was equally good in the fovea and the periphery. This represents a much steeper rate of sensitivity decline than the E_2 values of roughly 2.2 to 3 that Levi et al. recovered for a task of grating detection (Cowey & Rolls, 1974; Levi et al., 1985; Thibos, Still, & Bradley, 1996).

Saarinen (1988) employed *M*-scaling in a two alternative forced task (2AFC) where observers were required to discriminate between random or bilaterally symmetric dot clouds arranged across the horizontal axis presented out to 20º eccentricity. The experiment had two conditions, one in which the stimuli were presented at a constant size and one in which the stimuli were *M*-scaled with a value of 3 to compensate for decreasing ganglion cell density (based on Rovamo and Virsu's [1979] estimate for the nasal half of the horizontal visual field meridian). *M*-scaling proved inadequate to equate foveal and peripheral performance levels in the task although it did improve the percent

of correct responses over those generated with the un-scaled stimuli. In a subsequent study by Saarinen (1989) using a stimulus comprising two mirrored or translated S-shapes, *M*-scaling again failed to equate the percentage correct across the visual field for the observers. However, threshold target sizes, estimated from the data with a scaling value of approximately .77 as suggested by Levi et al., (1985) to represent the CMF, was sufficient to equate performance across the visual field.

A review of the *M*-scaling literature reveals that two sets of critical values have emerged from the results of spatial vision tasks performed with both primates and humans (Wilson et al., 1990). There is a range of E_2 of values on the order of 1.5º to 4º that include values for increasing cone receptor size, decreasing ganglion cell density (e.g., Dow et al., 1981), grating acuity and contrast sensitivity (Rovamo & Virsu, 1979). There is a second range corresponding to the CMF that is bounded by approximately .3º and .9º (e.g., Dow et al., 1981; Connolly & Van Essen, 1984). This range includes values for tasks of spatial positioning such as abutting vernier acuity (Levi et al., 1985) or optimal 2-dot vernier acuity (Westheimer, 1982, as cited in Wilson et al., 1990, p. 239).

Although *M*-scaling has been useful to delineate tasks that are limited by retinal factors from those that are limited by the CMF, there are some difficulties with this procedure. Most important, it is difficult to provide a solid estimation of the ganglion cell density in the fovea required for the estimation of E_2 (Rovamo & Virsu, 1979; Wilson et al., 1990). Secondly, there are considerable variations in both cone spacing and striate cortex area for humans and monkeys. A range of approximately 1500 to 3700 mm^2 has been found for both humans and the macaque monkey (Wilson et al., 1990). Therefore *M*-scaling makes assumptions about the architecture of the visual system that may not be

consistent across observers. To address the limitation of binding E_2 to anatomical loci S-scaling, or stimulus magnification, was introduced.

Stimulus Magnification and E_2

Stimulus magnification (also known as size scaling) refers to the determination of E_2 through psychophysical testing and involves presenting stimuli at a range of sizes and eccentricities across the visual field. If the visual system employs mechanisms that differ at each eccentricity only in terms of scale, meaning that the mechanisms get larger as eccentricity increases, then the performance versus size curves obtained at each eccentricity should differ only in terms of their positions on a log-size axis. In many cases the needed magnification (scaling) increases linearly with eccentricity so that if S_0 is stimulus size at fovea then in the function:

$$S_E = S_0 / (1 + E / E_2) \tag{3}$$

S_E is the stimulus size at eccentricity E required to elicit equivalent-to-foveal performance levels. E_2, in this procedure, is a task-dependent constant. In other words, S_E can be thought to represent the scale of the mechanisms at eccentricity *E,* relative to the scale of the mechanisms at fixation. Consequently, if stimulus size at eccentricity *E* is divided by S_E then the performance versus size curves at a range of eccentricities (*E*) should shift to the left and superimpose onto the foveal curve. This method is said to be assumption-free and studies that employ this type of methodology can be used to determine E_2 values to characterize eccentricity dependent changes for a variety of tasks.

A large number of assumption-free S-scaling studies have been produced and a variety of task specific E_2 values have emerged. The following are a small sample of E_2 values. Watson (1987) found an E_2 of 4.17 for contrast sensitivity in a task requiring the

detection of Gabor targets, which is higher than the scaling factor of 2.38 proposed for under-sampling (Rovamo & Virsu, 1979). A range of E_2 values from .58 to 2.07 with an average of ≈ 1º was found across various direction discrimination tasks employing point-light walkers (Gurnsey et al., 2008). These values are closest to the range proposed for limitations caused by the CMF (.3 to .9, see Wilson et al., 1990). Whitaker, Rovamo, MacVeigh and Mäkelä (1992) found a range of 1.66 to 1.83 for tasks of vernier acuity, larger by almost a factor of two than the estimation of .77 from the study by Levi et al. (1985). Mäkelä, Whitaker, & Rovamo (1993) found an E_2 value of about 1.95 for orientation discrimination, also higher than would be expected for a task of spatial positioning. Clearly there is a wide range of E_2 values that have been recovered for various tasks using the size scaling method. This thesis will add estimations for the detection and discrimination of symmetry in a crowded display.

Symmetry Detection Across the Visual Field

A great deal of work has been devoted to quantifying symmetry perception across the visual field (e.g., Barrett et al., 1999; Gurnsey et al., 1998a; Saarinen, 1988, Saarinen et al., 1989; Sally & Gurnsey, 2001; Tyler & Hardage, 1996; Tyler et al., 1995). Although symmetry is indeed present in many human artefacts and markings on wildlife, these studies have shown that sensitivity to mirror symmetry decreases in similar fashion to many other stimulus properties when it is presented away from the centre of the visual field. Symmetry detection tasks that use dynamic or static dot texture stimuli of varying densities (Barrett et al., 1999; Gurnsey et al., 1998a; Sally & Gurnsey, 2001, Tyler et al., 1995), or fine line stimuli (Saarinen et al., 1989) have recovered E_2 values for symmetry

discrimination that range from .47 to 1.22. These values are in a range commonly thought to relate to cortical limitations rather than retinal factors (Levi et al., 1985).

Barrett et al. (1999) asked how discrimination between perfect and varying degrees of imperfect symmetry might change as a function of visual field location. They used a seen/not-seen symmetry detection task and varied the size of the stimulus by varying viewing distance. Degradation of the pattern was achieved by first assigning one of the 256 grey levels to each of the 2 x 2 or 4 x 4 pixel blocks and then introducing new random grey levels in increasing proportions. The stimuli were presented at 2.5, 5, 7.5 and 10º eccentricity.

For one observer the E_2 value decreased from 1.15 for the 2 x 2 display to .91 for the 4 x 4 display and, for the second observer, E_2 values decreased from .65 to .57 respectively. Although the pattern of results was the same when the local pixel block size was increased from 2 x 2 to 4 x 4 (the standard deviation of the Gaussian window remained fixed at 33 pixels) the size versus sensitivity curves for the peripheral data were shifted to the left on the size axis (x-axis). This implies that discrimination becomes asymptotic at smaller target sizes when the pattern elements are larger. The average E_2 value ($\approx$ .8) is closest to the range thought to be limited by the CMF and is consistent with other studies of mirror symmetry in the periphery that find that sensitivity to mirror symmetry degrades at a rate which is comparable to positional acuity (Gurnsey et al., 1998a; Saarinen, 1989; Tyler and Hardage, 1995), and faster than the rate at which resolution degrades (Levi et al., 1985; Saarinen et al., 1988).

As previously mentioned, our ability to detect symmetrical targets depends somewhat on the amount of information around the axis or along the edges (Barlow &

Reeves, 1979; Jenkins, 1982). This suggests that we might need to fixate near the axis of symmetry for it to become salient. In many studies, the target location is always known to the observer (Barrett et al., 1999; Saarinen, 1989; Saarinen et al., 1988; Tyler & Hardage, 1996). A previous paper from Gurnsey, Herbert and Kenemy (1998a) found that detection accuracy (or d') decreased as a symmetrical target was moved farther from fixation whether the location was known or not. The target patch comprised 300 dots within a 200 by 300 pixel window (the dots were Gaussians within a 6 x 6 pixel window) presented at a variety of eccentricities up to approximately 40º to the left or right of fixation. There were three conditions, an *isolated* condition, and two other conditions in which the symmetrical stimulus was presented embedded in noise dots of the same density as the target but lacking the property of symmetry. In the *embedded/blocked* condition the eccentric location was known to the observer and in the alternate condition it was not (*embedded/unblocked*). Gurnsey et al. (1998a) measured accuracy for fixed stimulus sizes at a range of eccentricities, however the target sizes tested at 0º were not small enough to establish size-at-threshold. Using interpolated data they found that the E_2 values for the embedded/unblocked, embedded/blocked, and isolated conditions respectively were .46, .48 and 1.22.

A study by Sally and Gurnsey (2001) constructed stimuli to address the issue of whether or not there are mechanisms that detect *local* symmetry, in other words, the symmetry near the axis of symmetry, rather than the more remote information, provided by the outline contour of the stimulus. The symmetrical patches were surrounded by dots of the same size and density to obscure more global cues such as the contrast between the outer contour of the dot patterns and the empty background. The stimulus comprised

centre-surround Gaussian blobs (9 x 9 pixels) that were either in a random dot pattern or one that was symmetric about the vertical axis. The stimuli were presented across the visual field at eccentricities of 0 to 6º. On a given trial participants were required to report which of two briefly presented stimulus patterns contained the symmetrical target. Sally and Gurnsey found that at all eccentricities performance increased with stimulus size, E_2 values ranged from 1.38 to 2.03. These results sit at the high end of the range of E_2 values thought to represent spatial tasks that are limited cortically such as vernier acuity (Levi et al., 1985; Whitaker et al., 1992a) or orientation discrimination (Mäkelä, Whitaker, & Rovamo, 1993).

Previous estimates for tasks using symmetrical stimuli similar to those used by Sally and Gurnsey (2001) range from .47º to 1.22º (Barrett et al., 1999; Gurnsey et al., 1998a; Saarinen, 1988; Tyler & Hardage, 1996). Therefore, Sally and Gurnsey hypothesized that as visibility changes with stimulus size E_2, estimates may become inflated as the psychometric functions may represent a combination of limitations imposed by contrast sensitive mechanisms and those selective for symmetry (Poirier & Gurnsey, 1997). Stimulus contrast was constant in the first experiment and it was noted an E_2 of about 2.38º or greater should be required to compensate for acuity losses due to decreasing ganglion cell density in the periphery. Therefore, in a second experiment stimulus contrast was always set to four times detection threshold which brought E_2 values for both observers back into the range of cortical magnification limitations (1.26º and .88º), measured up to 8º eccentricity. (Note: Experiment 1 only went to 6º.) The E_2 values for contrast thresholds were ≈ 3.5º, consistent with E_2 values thought to represent acuity loss at a retinal level (e.g., Rovamo and Virsu, 1979). These results follow a

common pattern found in the symmetry literature that suggests there are two factors at play when scaling stimuli, resolution loss or visual under-sampling, and an eccentricity-dependent sensitivity loss due to limitations caused by the CMF (Barrett et al., 1999; Gurnsey et al., 1998a; Latham & Whitaker, 1996; Saarinen, 1988; Saarinen et al., 1989).

Vision scientists expect certain stimulus properties such as symmetry to '*pop out*' (draw attention) of a cluttered background in the same way that a blue B on a page of red B's would pop out, or an 'x' from among circles (Treisman & Gelade, 1980). In a visual search task when detection speed decreases with the number of elements in a stimulus (set size), target processing is thought to be serial rather than parallel. In other words, if symmetry is a property that '*pops out*' then it should be detected immediately (parallel search) without the observer having to scan the entire stimulus pattern (serial search). Olivers & Van der Helm (1998) provide evidence that mirror symmetry does not pop out of non-symmetrical distractors in a visual search task. The study comprised a series of tasks that examined four different categories of stimuli, a dot stimulus, an abstract pattern with a black outline, an abstract pattern filled in with black, and parenthesis pairs. Detection of the symmetrical target version of each category deteriorated with set size. These results suggest that symmetry does not alert the visual system to its presence. For another example of this effect see Gurnsey, Herbert and Nguyen-Tri (1998b).

In the study by Gurnsey et al. (1998a) the embedded/blocked condition (conditions described above) produced the same sharp performance decrease as the embedded/unblocked condition as stimuli were moved farther into the periphery, up to 40º eccentricity. It seems that location uncertainty was not a mitigating factor in decreased performance. Symmetry did not to seem to alert observers to its presence when

the location of the stimulus was unknown, neither did it pop out from the noise when the location was known. Barlow and Reeves (1979) also found that even when symmetrical targets are simply embedded in a random dot noise pattern, rather than being surrounded by competing stimuli as in a crowding study, detection begins to deteriorate as the axis of symmetry is moved farther from the mid-line into the periphery.

The results of the above studies show that symmetry is not as easily detected in the periphery as it is at fixation unless adequately size scaled. Even when size scaled it is not as easily detected from within a noisy display as it is when isolated (Gurnsey et al., 1998a; Sally & Gurnsey, 2001). Given these vulnerabilities it is possible that as separation between competing stimuli (flankers) and a symmetrical target decreases the ability to perceive that target accurately will also decrease. This is a phenomenon known as crowding and there is a large literature devoted to its characterization.

Crowding

The human visual experience most often requires that we select target objects for further processing from displays that are cluttered to varying degrees. Sometimes a target that is easily detected when presented in isolation becomes impossible to identify when surrounded by non-target features. This phenomenon is known as crowding and it is often studied using Gabor patches and alphanumeric stimuli (for review: Levi, 2008; Pelli, Palomaras, & Majaj, 2004; Whitney & Levi, 2011). Korte first characterized crowding in 1923 as "a pressure on both sides of the word that tends to compress it. Then the stronger, i.e., the more salient or dominant letters, are preserved and they 'squash' the weaker, i.e., the less salient letters, between them" (Translated by Uta Wolfe, as it appeared in Pelli et al., 2004, p. 1139). Since that time many questions have been debated in the literature in

an effort to establish a reliable and quantifiable characterization of crowding across the visual field. The following section will deal with precisely what crowding is, what it is not, and some of the assumptions of the phenomenon as defined by the empirical literature to date.

The characteristics of crowding.

Most crowding studies to date have found that crowding occurs only in the periphery (Bouma, 1970; Gurnsey, Roddy, & Chanab, 2011; Levi, Hariharan, & Klein, 2002a; Levi, Klein, & Hariharan 2002b; Strasburger, Harvey, & Rentschler, 1991). However, although the weight of evidence suggests that crowding is predominately a peripheral phenomenon there are exceptions in the literature that suggest that some tasks are subject to modest crowding effects at fixation (Danilova & Bondarko, 2009; Latham & Whitaker, 1996; Liu & Ariditi, 2000; Pelli et al., 2007). It has also been suggested that any crowding effects seen at fixation are simply a case of lateral masking (Levi et al., 2002a; Pelli et al., 2004; Strasburger, 1991). Therefore it is important to distinguish crowding from other forms of visual interference that can inhibit perception in a visual task.

Crowding versus Masking.

Overlap and lateral masking.

Although there are a number of sub-types of masking and suppression, we will deal with lateral (or overlap masking) and simple surround suppression here. Overlap or lateral masking is the type most often thought to produce what looks like crowding effects at fixation (Levi et al., 2002a). In overlap or lateral masking the targets and flankers abut or their edges slightly overlap. (Overlap masking differs from overlay

masking in which the target is overlaid on a mask - e.g., a suprathreshold grating.) According to Levi et al. (2002a) any 'crowding' effect seen at fixation is simply a case of lateral masking given that at the fovea crowding is scale invariant and proportional to target size, over a 50 fold range of target sizes.

There are a number of distinctions to be noted between crowding and masking, the following is an example of those distinctions relevant to the current study.

1. At fixation, the sizes and separations of crowded stimuli are often so small as to make it difficult to distinguish whether an effect is one of masking or crowding. Because crowding is largely defined by the smallest possible separation that can occur for targets to still be identifiable when surrounded by flankers (critical spacing), there is an assumption that crowding can only occur when targets and flankers do not overlap (Pelli et al., 2004). Also, the critical spacing in a crowding study can be ten times wider than a small signal and in this condition masking simply cannot occur (Bouma, 1970; Levi et al., 2002a; Toet & Levi, 1992).

2. Another distinction is that the masking effect is similar in the fovea and periphery while crowding seems to be predominantly a property of the periphery (Bouma, 1970; Levi et al., 2002a; Levi et al. 2002b). Also, the strength and extent of interference from flankers in the periphery is much greater for crowding than for masking (Levi et al., 2002b).

3. When a target signal is masked, it is suppressed and disappears thus affecting both detection and identification. In the case of crowding, the signal is visible but ambiguous, incorporating features from the mask (Flom, Weymouth, & Kahneman, 1963; Levi, 2008; Parkes, Lund, Angelucci, Solomon, & Morgan, 2001; Pelli, 2004).

4. It has been noted that any separation between target and mask (such as it might occur) scales with target size, independent of eccentricity (Levi et al., 2002a). This differs from crowding in that the critical spacing between flankers and targets is assumed to be approximately .5º of viewing eccentricity (Bouma, 1970; Toet & Levi, 1992), independent of target size (Levi et al., 2002a; Strasburger et al., 1991), mask size, number or relative contrast (Pelli et al., 2004; Strasburger et al., 1991).

Surround suppression.

Surround suppression is a form of neural suppression that occurs in physiological studies when a masking stimulus surrounds the receptive field of the target neuron and thus reduces the firing rate of the target neuron. Although surround suppression is strongest at eccentricities greater than 1º, a feature it shares with crowding (Petrov, Popple, & McKee, 2007), it is quite distinct. Most notably, surround suppression does not share with crowding the well-documented inward-outward anisotropy found in crowding studies that have used letter-like stimuli. That is, an alphanumeric flanker at an eccentric location will produce a greater crowding effect than one placed closer to fixation. This is due to the overrepresentation of the foveal region on the visual cortex that will actually cause the inner flanker to be a greater distance away in the neural representation (Bouma, 1970; Petrov et al., 2007).

Target size and target-flanker separation.

If peripheral vision were a linearly scaled version of foveal vision the effect of flankers on target detection would be of the same magnitude across the visual field. However, the evidence shows that when foveal and peripheral stimuli presented at peri-threshold size are surrounded with flankers of the same size, at separations proportional

to target size, there is greater disruption in the periphery than at fixation (Gurnsey et al., 2011; Pelli et al., 2004; Toet & Levi, 1992). Some studies have suggested that crowding is independent of target size (Levi et al., 2002a; Pelli et al., 2007; Strasburger et al., 1991) and further, that critical spacing is roughly half of viewing eccentricity thereby proportional to eccentricity (Bouma, 1970; Levi et al., 2002b; Pelli et al., 2004; 2007; Strasburger et al., 1991). If that is true, to maintain visual isolation of a target in the periphery (at any given eccentricity *E*) no other stimulus should be presented within a distance of about .5º*E* (Bouma, 1970).

Pelli et al. (2007) also tackled the issue of how size and separation might interact across the visual field. The question at hand was whether simply making the letters larger could increase reading rates or was it necessary to increase the separation as well. Each participant was briefly presented with a letter triplet drawn at random from ten characters ('DHKNORSVZ') of the Sloan font. The triplets were presented at a range of positions in the lower visual field (0 and 5º), and in the right visual field (0, 6 and 12º). The two flanking letters of the triplet were presented either to the right and left of the target, above and below, or diagonally at various locations around the target. Three letter sizes, scaled for eccentricity, were studied. Participants were required to identify the middle letter of any given trigram. 'Critical spacing' was measured as two opposing points on target and flanker (centre-to-centre).

With this method Pelli et al. (2007) were able to map out isolation fields for each observer. The term *isolation field* refers to the area within which features are integrated, from outer edge to outer edge of the triplet. It was found that the size of the isolation field was determined only by position in visual field and not by target letter size. They also

found that the regions of interference are elliptical in shape and oriented radially around the fovea. This result is consistent with previous work by Toet and Levi (1992) who used an orientation discrimination task using a letter 'T'. Toet and Levi found the same pattern of crowding regions as Pelli et al., out to 10º eccentricity, horizontally along the nasal meridian, vertically towards the lower visual field and diagonally (45º) in the lower visual field.

Although the general pattern of crowding is said to be elliptical in shape and oriented around the fovea, the pattern does not seem to be equally distributed across visual field meridian. He, Cavanagh and Intriligator (1996) found evidence of an anisotropy with respect visual field meridian and the effect of crowding in the upper visual field. He et al. asked participants to identify the orientation of a one cycle per degree test grating that was tilted either to the right (45º) or to the left (135º) of the vertical midline. Each patch subtended 2º with a 5º distance between the targets and flankers measured centre-to-centre. The stimulus was presented at four different contrast levels, alone for half of the trials and surrounded by four flankers of random orientation for the other half. The flankers were arranged horizontally, two on each side of the target, and the centre of the target was either 20º above or below the fixation point. When the target was isolated there was no anisotropy between the upper and lower visual field and participants responded with near perfect accuracy in both. However, when targets were crowded performance was severely degraded in the upper visual field (percent correct was roughly 56 to 63%) as compared to the lower visual field (percent correct was roughly 70 to 89%).

The crowding paradigms.

There are three commonly used paradigms used to study crowding.

1. The first employs a fixed target size that, when isolated, can be identified with a predetermined accuracy (e.g., 90%) by the observer. Then, the strength and extent of crowding can be measured by varying target-flanker separation and plotting percent correct versus flanker distance (e.g., Bouma, 1970; Chung, Li, & Levi, 2007).

2. The second assesses the influence of flanking stimuli on target discrimination by measuring a threshold value (e.g., contrast or target size) while various factors are manipulated such as the target-flanker configuration size and target-flanker distance. For example, an alphanumeric target such as a 'T' (Toet & Levi, 1992; Gurnsey et al., 2011), an 'E' (Levi et al., 2002a) or a Gabor patch (Poder, 2008; Poder & Wagemans, 2007) is surrounded by a number of flankers and the observer is required to report the orientation of the target, as stimulus size (Gurnsey et al., 2011; Latham & Whitaker, 1996), or target contrast (Parkes et al., 2001; Strasburger, 1991) is manipulated. Petrov et al. (2007) caution that studies using contrast threshold as a measure of performance may actually be measuring the effects of surround suppression when the flankers are of higher contrast than the target.

3. Finally, in studies of crowding and reading rate, two parametric measurements of letter identification are made. One measure is flanked acuity where the flank spacing is a multiple of the target size and the other a measurement of isolated letter acuity.

The present study will be placed in the second paradigm such that we will measure target size-at-threshold while the four factors, target-flanker configuration, size and separation, visual field location and orientation are manipulated.

Critical spacing and threshold determination.

Crowding is often described and quantified in terms of the critical spacing required to identify the target amongst flankers. It should be noted that some investigators characterize crowding in terms of the centre-to-centre separation between the target and flankers, while others characterize the distance (separation) between the closest edges. Regardless, many studies support Bouma's finding that critical spacing is ≈ .5*E* (Bouma, 1970; for review: Levi, 2008; Whitney & Levi, 2011). Studies such as these are also consistent with the notion that critical spacing represents a fixed distance on the cortex (Levi et al., 1985; Pelli, 2008). However, critical spacing is defined differently from study to study and further, it depends on how the performance threshold is determined.

Pelli et al. (2004) define critical spacing as the smallest separation between targets and flankers for which there is no threshold elevation as compared to the un-flanked condition. Tripathy and Cavanagh (2002) defined the extent of spatial interaction between targets and flankers in terms of the point on a fitted psychometric curve, with a lower asymptote set at 25%, that corresponds to a drop in the percentage of correct responses by a factor of 1/e (e = 2.718) from the upper asymptote of the un-flanked target condition. For example, if the amplitude of the fit (*A*) is 59.1% when flankers are present, and the upper asymptote is 84.1% in the un-flanked condition, then the extent of the interaction corresponds to a percentage of correct responses calculated as

$$A(1 - 1/e) + 25\% = 62.4\% \quad (4).$$

Critical separation then is the target-flanker separation yielding 62.4% discrimination accuracy. As a final example, Toet and Levi (1992) used both interpolation and Probit analysis (a type of regression used to analyze binomial response variables) to determine

the distance between the midpoints of the two vertical bars of two adjacent 'T's that results in a drop from ceiling level orientation discrimination to 75%. This was considered to be the zone of interaction, or the distance at which a target becomes crowded.

Given the discrepancy between methods of threshold determination, Gurnsey, Roddy and Chanab (2011) following Latham and Whitaker (1996) approached the crowding issue with the view that the extent of interaction zones should be viewed as continuous in nature. Because interference zones have been shown to increase with eccentricity at a far greater rate than that of resolution thresholds when targets are crowded (Latham & Whitaker, 1996; Toet & Levi, 1992), Gurnsey et al. sought to place the crowding issue into a framework of double scaling based on a range of sizes and eccentricities to fully characterize the rate at which the zone of interaction increases across the visual field.

Although single linear magnification functions are often sufficient to compensate for eccentricity-dependent acuity loss (Weymouth, 1958), some tasks, such as face or subjective contour perception, seem to have multiple eccentricity-dependent sensitivity losses that require multiple linear magnifications to equate performance across the visual field (Latham & Whitaker, 1996; Melmoth, Kukkonen, Mäkelä, & Rovamo, 2000; Poirier & Gurnsey, 2002; Toet & Levi, 1992). For example, in a task of face identification Melmoth, Kukkonen, Mäkelä, and Rovamo, (2000) found that contrast had to be scaled at a different rate than target size in order to equate performance levels at 10º eccentricity to those obtained at fixation. In other words, size and contrast required different E_2 values to

characterize sensitivity loss (Melmoth et al., 2000). It is possible that symmetry might also require a double scaling procedure.

Latham and Whitaker (1996) and Gurnsey et al. (2011) suggest that critical spacing should not be defined by an arbitrary choice of threshold to determine when targets have become crowded. In the study by Latham and Whitaker (1996), observers were asked to discriminate the orientation of a target grating that was either isolated, or flanked above and below, or left and right. They determined the stimulus size required to achieve a threshold of 75% correct in a 2AFC. Threshold was obtained at edge-to-edge separations of 0.25 to 7 times target size (corresponding to centre-to-centre separations of 1.25 to 8 times target size) at each of four eccentricities (0, 2.5, 5, and 10º). With this method Latham and Whitaker (1996) were able to express the critical separation (s_{crit}) needed to achieve a particular threshold elevation (T_{rel} = flanked vs. un-flanked size threshold) at any given eccentricity (E) in terms of two free parameters:

$$s_{crit} = \frac{s_2 / E_{2H}}{T_{rel} - 1}(E = E_{2H}) \tag{5}$$

where s_2 is the separation at fixation at which size (resolution) threshold is twice the un-flanked threshold, and E_{2H} is the eccentricity at which the separation eliciting T_{rel} doubles. Clearly, s_{crit} will be proportional to eccentricity when E_{2H} / E is small, but the exact proportion depends on T_{rel}. The Latham and Whitaker approach provided the model for a previous study in this lab (Gurnsey et al., 2011, method described below) and the two studies combined will provide the base from which the current study will begin its investigation. The analyses used in these two studies suggest that critical separation may be proportional to eccentricity but the exact proportion depends on the threshold

elevation used to define critical separation.

Crowding and Symmetry Across the Visual Field

Many stimulus properties are subject to the effects of crowding even when magnified and they include simple discrimination of letter targets (Pelli et al., 2004) and fine discrimination of the contrast, spatial frequency, and orientation of Gabor patches and other alphanumeric stimuli (e.g., Levi et al., 2002a; Levi et al., 2002b; Parkes, et al., 2001; Toet & Levi, 1992). It has been found that observers are often able to discriminate a briefly presented isolated symmetrical dot pattern from a random one at any position in the visual field if it is sufficiently magnified (Barlow & Reeves, 1979; Gurnsey et al., 1998a; Jenkins, 1982; 1983; Saarinen, 1988; Tyler, et al. 1995; Wenderoth, 1994). It is therefore useful to ask whether stimulus magnification will be adequate for symmetry discrimination when the symmetrical target is crowded.

Previous crowding studies have sought to quantify the rate at which the zone of interference increases across the visual field and to examine whether the periphery differs only in scale or is qualitatively different from the foveal region (Gurnsey et al, 2011; Latham & Whitaker, 1996; Toet & Levi, 1992). Symmetrical targets have not been widely studied in this context. Experiment 1 will investigate the vulnerability of symmetry discrimination to the effects of crowding across the visual field within a framework of multiple scaling (as per Gurnsey et al., 2011 and Latham & Whitaker, 1996). To accomplish this, configurations are created with targets (symmetrical patches) flanked by non-symmetrical flankers at a range of separations that are proportional to target size. The size of an entire configuration is varied across trials until the target size eliciting a fixed level of discrimination accuracy is obtained. In this way the target size-

at-threshold and the target-flanker separation-at-threshold can be simultaneously determined.

As previously noted, early work on symmetry perception in the vision science literature typically considered symmetry to be a highly salient image feature of our visual world (for review: Wagemans, 1995) that can be detected even in degraded form (Barlow & Reeves, 1979; Barrett et al., 1999; Gurnsey et al., 1998a; Saarinen, 1988). However, evidence showing that mirror symmetry does not pop out of non-symmetrical distractors in a visual search task (Gurnsey et al, 1998b; Olivers & Van der Helm, 1998) and that it is difficult to detect when surrounded by random noise in the periphery (Gurnsey et al, 1998a) suggests that symmetry/non-symmetry contrasts are not special to the early visual system. Previous work in this lab using alternate stimuli has shown that target size-at-threshold increases at a modest rate in the absence of flankers (Gurnsey et al., 2011). However, the presence of flankers increases the rate at which target size thresholds increase with eccentricity, the smaller the separation the greater the rate of that increase (Gurnsey et al., 2011; Latham & Whitaker, 1996; Toet & Levi, 1992). If symmetry is not processed in parallel by the early visual system we might expect to see size thresholds increase at a much faster rate in the presence of flankers than in their absence (Gurnsey et al, 2011).

Experiment 1 will use the method outlined by Gurnsey et al. (2011) to ascertain whether symmetry shares with other stimuli, such as gratings or letters, the common characteristics of crowding:

1. The general consensus is that crowding occurs only in the periphery and that any crowding effects seen at fixation are likely masking (Bouma, 1970; Gurnsey et al.,

2011; Levi et al., 2002a, Levi et al., 2002b; Strasburger et al., 1991). If symmetry is special to the visual system, or if there are specialized mechanisms for its detection, size thresholds should increase at a much faster rate in the presence of flankers than in their absence.

2. There is the possibility that the magnitude of spatial interference will increase with eccentricity and it is therefore pertinent to ask whether single or multiple, linear or nonlinear, magnification factors are required to characterize performance across the visual field. Symmetry may well possess properties that will require more than one magnification factor such has been found for tasks of face or subjective contour perception (Melmoth et al., 2000 and Poirier & Gurnsey, 2002 respectively).

3. By placing the flankers in both a horizontal and vertical configuration around the target in each of two visual fields, the lower visual field (LowerVF) and the right visual field (RightVF), we can investigate whether there will be an anisotropy with respect to target-flanker configuration or visual field meridian. We can also ask if the regions of interference will follow the pattern suggested by Pelli et al. (2007) and Toet and Levi (1992). In other words, it is possible that in the lower visual field vertically oriented flankers will cause greater interference than horizontally oriented ones and in the right visual field the horizontally oriented flankers will cause greater interference than vertically oriented ones.

4. It is also possible that we will find the presence of an anisotropy with respect to visual field meridian. He et al. (1996), found greater disruption in the upper visual field as compared to the lower visual field when targets were crowded. When the target was

isolated the anisotropy disappeared and participants responded with near perfect accuracy in both fields.

Method-Experiment 1

Participants

The participants included one of the authors (GR), a female, and one male naïve participant (WC). Both had normal or corrected-to-normal vision, as assessed by the Freiburg acuity test (Bach, 1996). Acuity was tested once at the beginning of the experiment from a viewing distance of 400 cm.

Apparatus

The experiments were conducted using an Intel MacPro Computer equipped with a ViewSonic G225f 21-inch multi-scan monitor with the refresh rate set to 85 Hz and pixel resolution set to 2048 horizontal by 1600 vertical. Pixel size was approximately .188 mm. All aspects of stimulus generation, presentation and data collection were under the control of MATLAB (Mathworks, Ltd.) and the Psychophysics Toolbox extensions (Kleiner, Brainard, & Pelli, 2007). A chin rest was used to help the participants maintain a steady gaze on the fixation dot.

Stimuli

The stimuli were 7 x 7 arrays of black and white checks. The target arrays were symmetrical about the vertical or horizontal axes and flanker arrays were randomly black and white. Figure 1 provides an illustration of targets and flankers and the configurations in which they were presented. Targets could be flanked horizontally (flankers to the left and right of the target on the midline) or vertically (flankers above and below the target) with a centre-to-centre separation of 1.25, 1.70, 2.32, 3.16, 4.31, 5.87, or 8.00 times target size. There was also an un-flanked condition. Stimulus configurations were presented at 0, 1, 2, 4, 8 and 16° eccentricity in the RightVF or LowerVF. Stimulus

target-centres were always presented in the centre of the screen. Varying viewing distance and the position of a fixation dot controlled the eccentricity of stimulus presentation. Viewing distances varied from 40 to 456 cm and were chosen to satisfy the twin constraints of (a) keeping the fixation dot and stimulus on the screen and (b) maximizing the number of pixels per check. For example, stimuli presented at fixation were always viewed from 456 cm and those presented at 16° were viewed from 40 cm. In all cases the luminance of the gray background region was 42.28 cd/m^2. The luminance of the target (and flankers) was 3.1 cd/m^2 for the black checks and 107.8 cd/m^2 for the white, which produces a Michelson Contrast of .944.

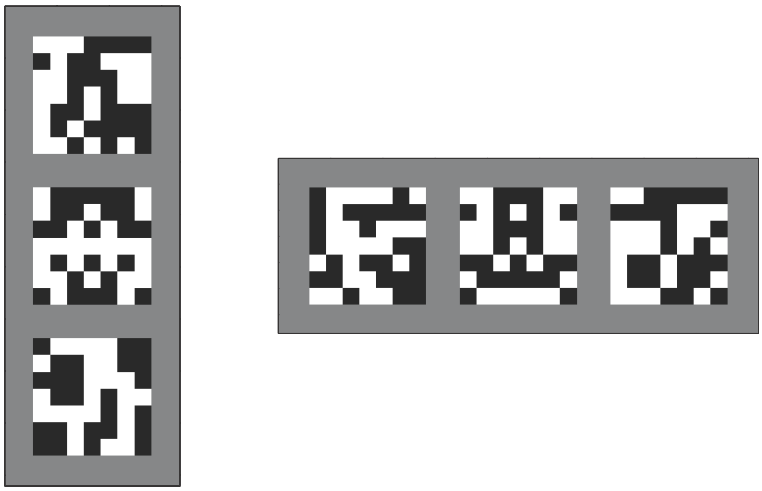

Figure 1. Trigrams used for Experiment 1. The central element (target) was a symmetrical patch that could have a vertical (shown) or horizontal axis of symmetry. The flankers could be above and below (left trigram) or to the left and right of the target (right trigram). The entire configuration (trigram) could be parallel to or perpendicular to the line that connects the central target to the point of fixation.

Procedure

On each trial of the experiment the participant's task was to report whether the symmetrical target patch (centre of the trigram) was horizontal or vertical. Two non-symmetrical flankers flanked the symmetrical target at one of the seven relative separations. There was also an un-flanked condition. The Quest adaptive procedure (Watson & Pelli, 1983) adjusted the size of the entire stimulus (target + flankers) on the basis of the participant's response history; stimulus size was decreased during periods of correct responses and increased during periods of incorrect responses. The goal of the adaptive procedure was to find the target size that elicited 81% discrimination accuracy in the two-alternative forced choice task (2AFC). The adaptive procedure ran until the standard deviation of the threshold probability density function fell below .05, or 100 trials, whichever came first.

A small green fixation dot was placed either above (for stimuli in the LowerVF) or to the left (for stimuli in the RightVF) of the stimulus except at 0º eccentricity, in which case the participant fixated the stimulus. The stimulus was presented for 333 ms, after which the participant entered his or her response; the up-arrow for a vertically symmetrical stimulus and either of the side arrows for horizontally oriented symmetry. Incorrect responses were signalled by a 300 ms, 400 Hz tone.

There were four factors in the experiment: Visual Field (RightVF and LowerVF), Flanker orientation (horizontal or vertical), Eccentricity (0, 1, 2, 4, 8 and 16°) and Relative Separation (1.25, 1.70, 2.32, 3.16, 4.31, 5.87, 8.00, and ∞ times target size-the un-flanked condition). For each of these 192 conditions three thresholds for each combination of size and eccentricity were obtained and then averaged. Consequently,

each participant produced 576 thresholds, each of which required 2 to 3 minutes to obtain. Each of the four combinations of Visual Field and Flanker Orientation were tested in random order. The conditions were not interleaved, such that each block contained only one condition at a time. For example, a participant would respond to presentations of a horizontally aligned trigram in the RightVF at all combinations of size and separation from widest to narrowest, at all eccentricities from 0 to 16º in that order, before proceeding to the next condition. Prior to data collection participants received sufficient practice to become familiar with the task.

Results-Experiment 1

The top two rows of Figure 2 plot the results for the two participants. The bottom row depicts target size thresholds averaged across participants. In each panel the y-axis represents target size-at-threshold (in degrees visual angle) and the x-axis represents target-flanker separation in multiples of target size (relative separations). Thresholds are plotted as a function of relative, centre-to-centre, target-flanker separation for eccentricities 0, 1, 2, 4, 8 and 16º eccentricity. Columns 1 and 2 represent flankers that are horizontally configured (parallel to the x-axis) about the target in the right and lower visual fields respectively. Columns 3 and 4 represent flankers that are vertically configured (parallel to the y-axis) in the right and lower visual fields respectively. Each line of data points represents an eccentricity (e.g., blue circles represent 0º) as denoted by the legend. The first seven data points represent conditions in which relative separations were 1.25, 1.70, 2.32, 3.16, 4.31, 5.87, or 8.00 times target size. The triangular data point in the right of each panel represents the un-flanked condition (plotted at 16 times target size for illustration).

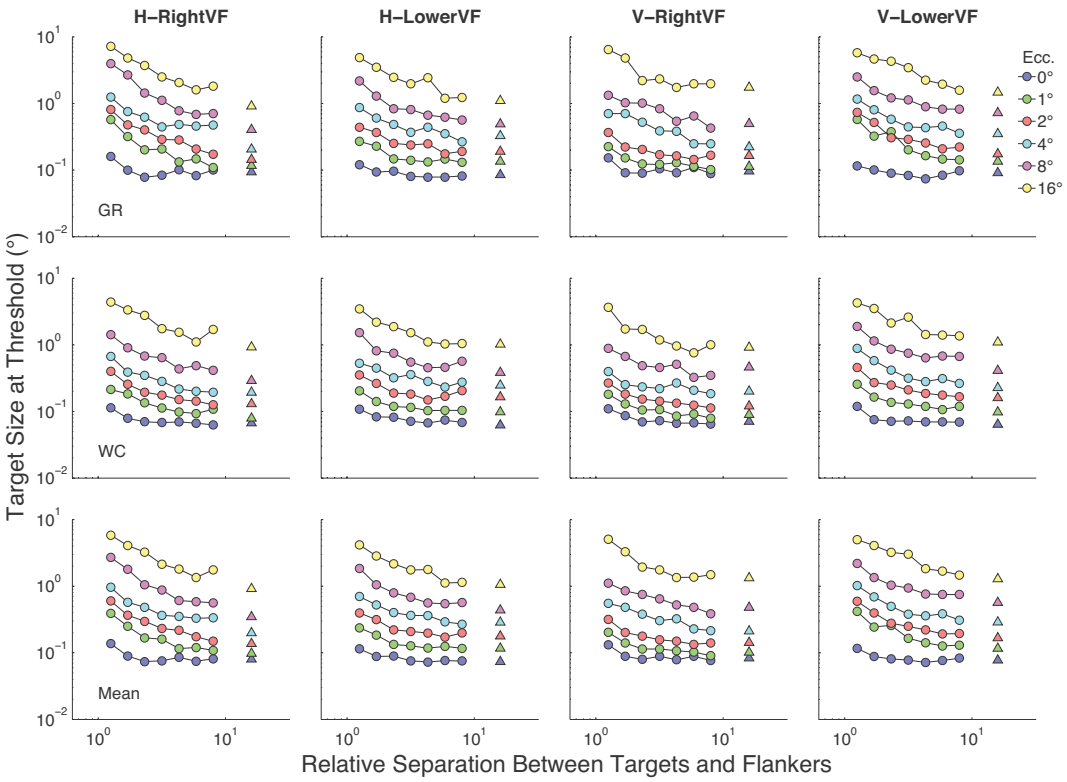

Figure 2. Target size-at-threshold as a function of the relative separation of targets and flankers plotted at each eccentricity. Rows 1 and 2 plot results for GR and WC respectively and Row 3 plots mean results. Columns indicate condition: the four combinations of flanker positions with respect to the target (horizontal and vertical) and position in the visual field (RightVF and LowerVF). Circles indicate separation of 1.25 to 8 times target size and the triangles at right in each panel represent the un-flanked condition depicted at 16 times target size for illustration. Circle colours represent eccentricities of 0 to 16º (see legend).

Figure 3 plots size threshold as a function of absolute separation-at-threshold (Relative separation * Target size). At fixation (blue symbols, 0º), size thresholds are largely independent of target-flanker separation with a modest increase over the un-flanked condition, at the two smallest separations. At all other eccentricities, threshold elevation is considerably greater at the smallest sizes and decreases as separation increases until asymptote is reached at the largest separations. Although there is some noise in the present data set, curves are generally shifted up and to the right as eccentricity increases. The continuous curves show the best fitting rectangular parabola, the procedure for which is explained in detail below. The small gray point at the upper end of each curve represents the point on the curve for which size-at-threshold equals separation-at-threshold (also explained below). At all eccentricities target size-at-threshold decreased as target-flanker separation increased. The upward shifts of the curves correspond to changes in the un-flanked size thresholds as the result of resolution loss. The rightward shifts correspond to the rate of increase of the separation between target and flankers.

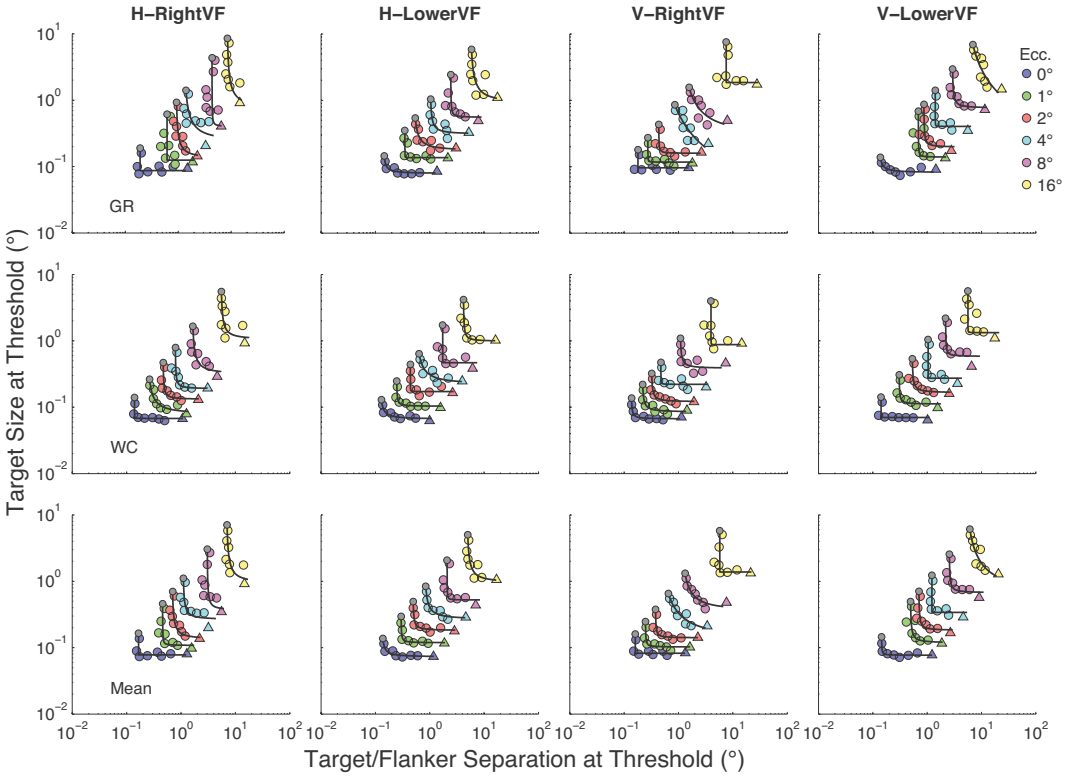

Figure 3. Size-at-threshold plotted as a function of the absolute separation of targets and flankers at threshold. (Target-flanker separation-at-threshold = target size-at-threshold * relative separation.) Rows and columns are arranged as in Figure 2. Circles represent target-flanker separations of 1.25 to 8 times target size at each eccentricity. Triangles represent the un-flanked condition at each eccentricity. The continuous curves show the best fitting rectangular parabola; see results section for details. The small gray point at the upper end of each curve represents the point on the curve for which size-at-threshold equals separation-at-threshold (see text for details).

At small separations, the upper portion of the curves at 1, 2, 4, 8, and 16º eccentricity become parallel to the y-axis and at larger separations they tend to asymptote parallel to the x-axis. When the separation vs. size curve is parallel to the y-axis separation-at-threshold is independent of target size. In other words, the centre-to-centre separation between targets and flankers remains the same despite changes in target size. The part of the curve that is parallel to the x-axis indicates that size thresholds are independent of target-flanker separation. In these cases, threshold is limited by target size and is independent of the centre-to-centre separation between targets and flankers. In other words, flankers have no influence on size thresholds. Between these two extremes (0 and 90º) separation-at-threshold increases as stimulus size-at-threshold decreases. To fully characterize decreasing sensitivity to symmetry in a crowded display, across the visual field, five analyses were attempted and are described in detail below.

Poirier & Gurnsey (2002): Double Linear Scaling Method

A prominent feature of Figure 3 is that the psychometric functions go from parallel to the x-axis at fixation to increasingly steep as eccentricity increases. For the four conditions there appears to be very little crowding at fixation (size thresholds are independent of target-flanker separations) to increasing crowding beginning at 1° (separation-at-threshold gets closer to target size independence). Therefore, one conclusion might be that the curves change shape with eccentricity and are simply *not* shifted versions of each other as has been previously suggested (Latham & Whitaker, 1996; Poirier & Gurnsey, 2002). On the other hand, it can be argued that the functions at each eccentricity represent samples taken from different sections of the same underlying

curve. Therefore, it should still be possible to shift curves from all eccentricities onto a single curve.

As in Gurnsey et al. (2011), we employed a modified version of the data fitting procedure first described by Poirier and Gurnsey (2002). The data at each eccentricity are assumed to conform to a rectangular parabola:

$$c^2 = (sep - sep_{min})(size - size_{min}) \quad (6).$$

At fovea *size* and *sep* are stimulus size and target-flanker separation-at-threshold, respectively. The limiting size-at-threshold at which the parabola becomes parallel to the separation-axis (i.e., the size eventually reached in the no-flanker condition) is $size_{\min}$, and $sep_{\min}$ is the limiting separation-at-threshold at which the psychometric function becomes parallel to the size-axis (i.e., the smallest centre-to-centre separation for which targets and flankers do not overlap, which is equal to 1).

We can rearrange Equation 6 to express *sep* and *size* in terms of the three parameters that describe the parabola ($c^2, size_{\min}, sep_{\min}$),

$$sep = \frac{c^2}{(size - size_{min})} + sep_{\min} \quad (7)$$

and

$$size = \frac{c^2}{(sep - sep_{min})} + size_{\min} \quad (8).$$

Equations 7 and 8 can also be expressed with fewer characters:

$$a = \frac{\gamma}{(b - \beta)} + \alpha \quad (9).$$

If we know that the relationship between *a* and *b* is

$$a = \mu b \tag{10}$$

then a and b can be expressed strictly in terms of the parameters of the parabola and the known relationship between *a* and *b*,

$$a = \frac{1}{2}(\sqrt{a^2 - 2\alpha\beta\mu + \beta^2\mu^2 + 4\gamma\mu} + \alpha + \beta\mu) \tag{11}$$

and

$$b = \frac{(\sqrt{a^2 - 2\alpha\beta\mu + \beta^2\mu^2 + 4\gamma\mu} + \alpha + \beta\mu)}{2\mu} \tag{12}.$$

If *x* and *y* are observed data points, then *a* and *b* are predictions of *x* and *y* based on $\mu = x / y$, α, β and γ (parameters of the rectangular parabola). We can then calculate the squared Euclidean distance (computed on the logarithms of *x*, *y*, *a* and *b* in order to reduce variability in the distance errors) between these two pairs of points along a line with slope $\mu = x / y$ emanating from the origin. This method was also used to find the best fitting rectangular parabolas for our data in Experiments 2a and 2b.

By assumption curves at any eccentricity can be shifted onto the foveal curve by dividing size (or separation) by the appropriate scaling factor $1 + E / E_2$,

$$Size_{Scaled} = \frac{Size}{1 + E / E_{2V}} \tag{13}$$

and

$$Sep_{Scaled} = \frac{Sep}{1 + E / E_{2H}} \tag{14}.$$

An error minimization procedure (fminsearch) can then be used to find the best fitting values for $c^2, sep_{\min}, size_{\min}, E_{2V}$ *and* E_{2H}. The best fitting rectangular parabola (defined

by the best fitting values of $c^2, sep_{\min}, size_{\min}$) describes all combinations of size and separation eliciting threshold performance. For simplicity we will report the values k_V and k_H which are the reciprocal values of E_{2V} and E_{2H} respectively. As previously mentioned, *k* describes the rate of sensitivity loss with increasing eccentricity, therefore smaller numbers refer to slower sensitivity loss and as the values increase so too does the rate of magnification. Figure 4 shows the results of dividing size-at-threshold by $1 + k_V E$ and dividing separation-at-threshold by $1 + k_H E$.

The downward shifts (k_V) account for visual under-sampling and suggest a rate of magnification for the conditions H-RightVF, H-LowerVF, V-RightVF, V-LowerVF of .4, .68, .43 and .75 respectively (averaged across participants). These k_V values are similar to other results such as those of Latham and Whitaker (1996) who found an average *k* of .71 in the lower visual field in the un-flanked condition for an orientation discrimination task. Gurnsey et al. (2011) found k_V values in the lower visual field of .57, .74 and .54 for a 4AFC 'T' orientation task, a 10AFC letter identification task and a 2AFC grating orientation task respectively.

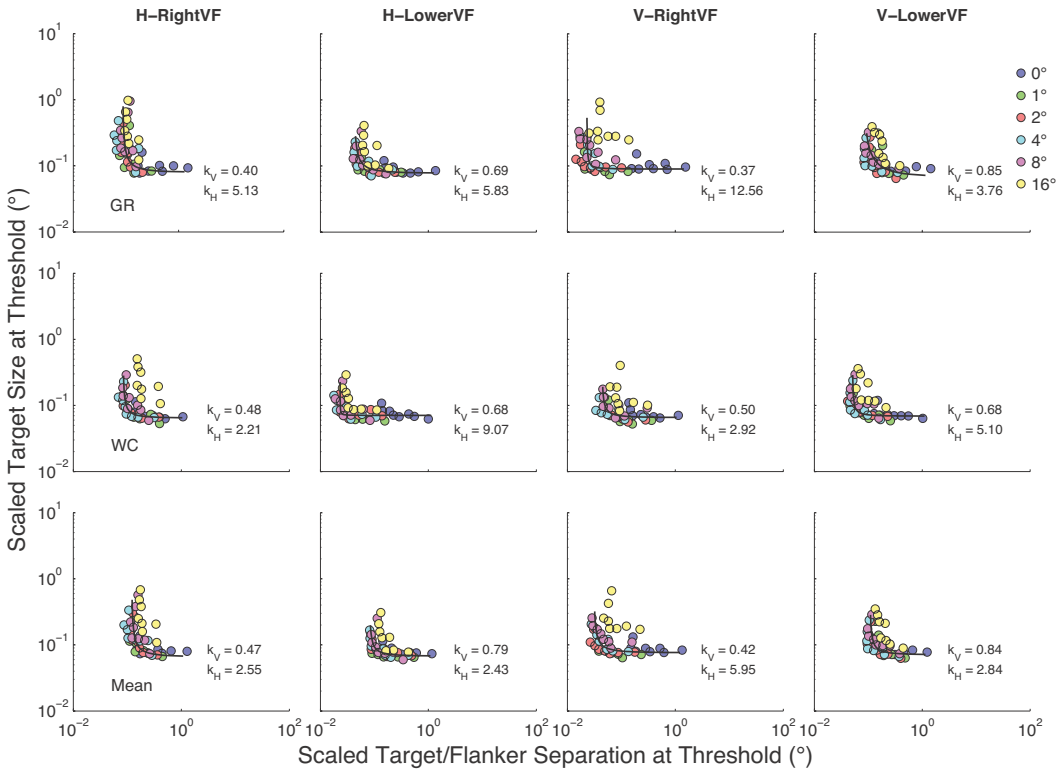

Figure 4. Poirier & Gurnsey (2002): Double Linear Scaling Method**.** These panels describe the data when collapsed onto the foveal standard using two linear magnification factors (see results section for details). Rows and columns are arranged as in Figures 2 and 3. Circles represent target-flanker separations of 1.25 to 8 times target size at each eccentricity. The k_V and k_H values for each condition are noted in each panel.

In the present study the k_V in the right visual field produced values of .44 and .43 (averaged across participants) for the horizontal and vertical conditions respectively. These values are consistent with values in a range thought to represent acuity loss at a retinal level (≈ .42) (e.g., Rovamo and Virsu, 1979; Saarinen et al., 1988). However, the k_V values in the lower visual field (.68 and .76 for the horizontal and vertical conditions respectively) are higher than those of the LowerVF.

To characterize the rate at which target-flanker separation must increase with eccentricity to equate visual performance, the leftward shift (k_H) produced values of 2.38, 7.45, 7.74, and .4.43 (averaged across participants) for conditions H-RightVF, H-LowerVF, V-RightVF and V-LowerVF, respectively. These values, along with those for k_V as noted previously, are consistent with the suggestion that target size-at-threshold increases more quickly in the presence of flankers than in their absence (Gurnsey et al., 2011; Latham & Whitaker, 1996).

The fits are generally quite good when eccentricity is included as a source of variability. Table 1 depicts r^2 values by condition (rows) across fitting procedure (primary column headings) for both participants (GR and WC, secondary column headings). The conditions refer to a horizontal configuration of target and flankers in the right and lower visual fields (HRVF and HLVF respectively) and a vertical configuration in the right and lower visual fields (VRVF and VLVF). The fitting procedures refer to Poirier & Gurnsey (2002): Double Scaling method and :Linear/Nonlinear Scaling Method (PG1 and PG2 respectively), and Gurnsey et al., 2011: 'Raw' Scaling Method, : two linear scaling factors and : two nonlinear scaling factors (Raw, LL, NLNL respectively).

Please note that only PG1 has been addressed thus far. Each fit will be discussed separately in the following sections. Row 7 provides the mean r^2 value for each fitting procedure for each participant across conditions and row 8 provides the mean r^2 value for each fitting procedure overall. The proportion of variability explained by the un-scaled data (r^2), which includes eccentricity as a source of variability, was quite good at .95 (Row 8, first column). For comparison Table 2 provides the r^2 values associated with the scaled data. All columns and rows are configured exactly as in Table 1. For the current method (double linear scaling) r^2 = .71 (Table 2, Row 8, first column), which is a far worse fit than the .95 obtained for the un-scaled data.

The double scaling method produced good fits when eccentricity was included as a source of variability. However, there was a considerable decrease in the r^2 value when the data were scaled. This trend was especially noticeable in the horizontal configuration in the RightVF where the r^2 values decreased from .96 to .52, and the vertical configuration in the LowerVF where the average r^2 value is .98 for the un-scaled data as compared to .55 for the scaled data. The degraded fits apply to the conditions that are representative of the pattern commonly thought to represent crowding regions, elliptical in shape and oriented towards the fovea (Pelli et al., 2004; Toet & Levi, 1992). In other words there was more variability when targets were flanked vertically rather than horizontally in the lower visual field and horizontally rather than vertically in the right visual field (Fig. 9).

Figure 4 makes clear that the leftward shift of the psychometric curves, as characterized by the k_H values, has produced an unsatisfactory fit with respect to the data at 16º (yellow circles). Note that in most cases the yellow dots (representing data from

16°) are to the right of the best fitting line. This suggests that a linear horizontal shift fails to capture the way in which crowding changes with eccentricity.

There is a second failure of the double linear fit that may not be immediately obvious from visual inspection. The best fitting functions (solid continuous lines) predict stimulus configurations at fixation that violate assumptions about what constitutes crowding, namely, crowding only exists for $separation_E / size_E$ ratios of 1 or greater. In other words, when the data are shifted leftward the separation at fixation required to match the maximum observed size-at-threshold at 16° is less than target size, and thus $separation_E / size_E$ is considerably smaller than 1. These points are represented by the left ends of the best fitting functions in Figure 4 and range from .000029 to .59. Therefore, whatever the quality of the fits might be, they violate assumptions of crowding, and are more likely to be placed in the rubric of masking (e.g., Levi, 2008; Pelli et al., 2004; Whitney & Levi, 2011).

The preceding point can be made in a different way. The grey dots in each panel in Figure 3 show that at fixation the maximum possible elevation of size-at-threshold is far less than the maximum possible elevation at 16°. The percentage increase over the un-flanked condition was between 27 and 72% at fixation (0º) for participant GR and between 56 and 86% for participant WC. However, at 16º the percentage increased from 291 to 697% for GR and 243 to 377% for WC.

One may ask why the error minimization procedure has converged on the implausible fits shown in Figure 4. There are two related reasons. First, because the target-size thresholds at fovea (0º, blue dots in Figure 3) show almost no dependence on target-flanker separation and they do not constrain the leftward shift of the curves.

Secondly, the curves are simply irreconcilable. The requirement for a *linear* leftward shift makes it impossible for the leftmost component of each shift to align at a plausible point while minimizing error. Therefore, in our next analysis we examine a non-linear leftward shift.

Poirier & Gurnsey (2002): Linear/Nonlinear Scaling Method

The assumption that the required leftward shift is a linear function of eccentricity may not hold because separation-at-threshold appears to increase non-linearly across the visual field. Figure 4 made clear that the data at 16º could not be captured by two linear scaling factors. In most cases the data points were well to the right of the best fitting curve. In other words, the required leftward shift seems to accelerate with eccentricity, implying a quadratic component to the fit. Therefore, we sought to characterize the extent of crowding, or the range of interference zones, across the visual field using non-linear multiple magnification. A second fit was undertaken with Equation 13 replaced by Equation 15 to accomplish the horizontal shift:

$$sep_{Scaled} = \frac{sep}{1 + E^{\alpha} / \beta} \tag{15}$$

where α and β are free parameters that work together to allow the degree of the leftward shift to increase non-linearly and better describe the change in the magnitude of crowding across eccentricity. We used the MATLAB error minimization procedure (fminsearch) to determine the values of $c^2, sep_{\min}, size_{\min}$, α and β that provided the best fit to the data (see Gurnsey et al., 2011) (Please note that α and β here bear no relation to α and β in Equations 8-11 of this paper). The results of this analysis are summarized in Figure 5.

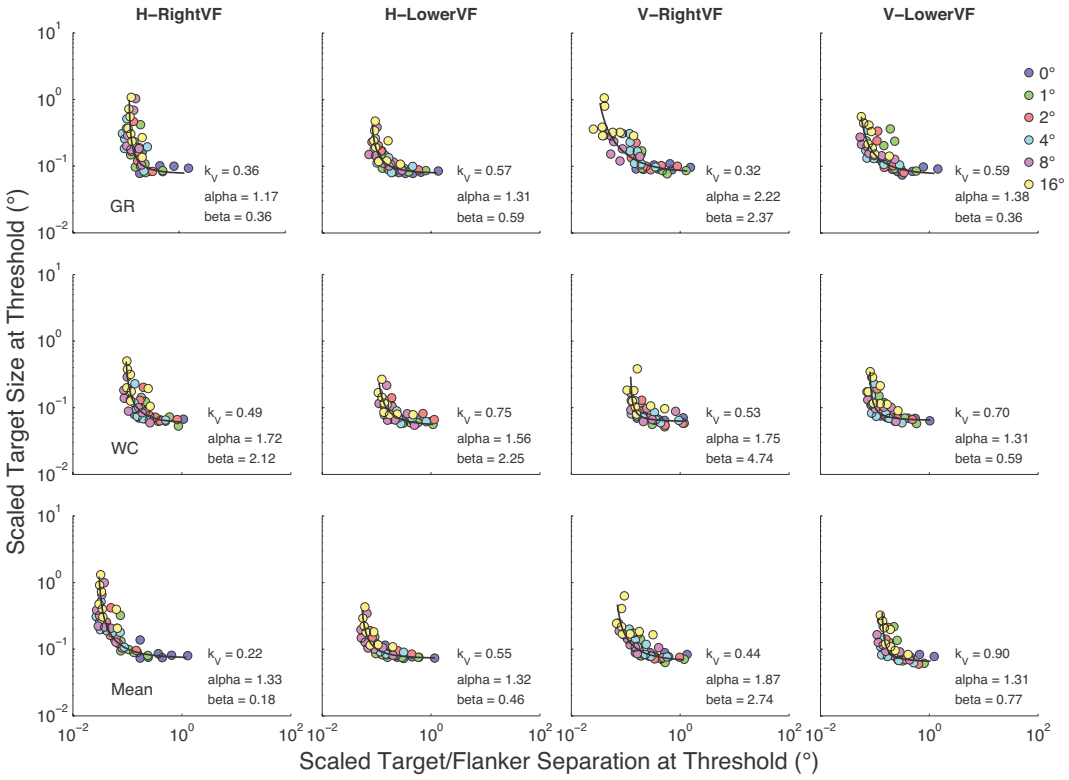

Figure 5. Poirier & Gurnsey (2002): Linear/Nonlinear Scaling Method, describes the data when collapsed onto the foveal standard using one linear- and one non-linear- magnification factor. Rows and columns are arranged as in Figures 2 to 4. Circles represent target-flanker separations of 1.25 to 8 times target size at each eccentricity. The continuous black line represents the best fitting rectangular parabola; see results section for details. k_V, α and β for each condition are noted in each panel.

Figure 6 depicts the magnification or scaling factors as a function of eccentricity. The slope of the required downward shift (Eq 12), which characterizes the rate of resolution loss, is relatively shallow across the visual field. For the conditions H-RightVF, H-LowerVF, V-RightVF and V-LowerVF the procedure produced k_V values (averaged over participants) of .42, .66, .42 and 1.29 respectively. Thus, the results are still consistent with those of Latham and Whitaker (1996) and Gurnsey et al. (2011). The k_V values are also in line with Gurnsey et al. (1998a) who found a k_V value of .82 in their isolated condition.

It is interesting that Gurnsey et al. (1998a) used single symmetrical targets embedded in random dots of the same density while ours were surrounded by interfering flankers. Yet the k_H values in the Gurnsey et al. study for the embedded/blocked and embedded/unblocked conditions (2.17 And 2.08 respectively) and the k_H values for the double linear fit in the present study (an average of ≈ 5.5) are much higher than the suggested rate of magnification for tasks of positional acuity (≈ 1.30, Levi et al., 1985). This provides further evidence that the magnitude of crowding increases with eccentricity.

The α and β values, which represent the combined effects of minimum size and separation were for α, 1.33, 1.32, 1.87, 1.31 and for β, .18, .46, 2.74, .77 respectively.

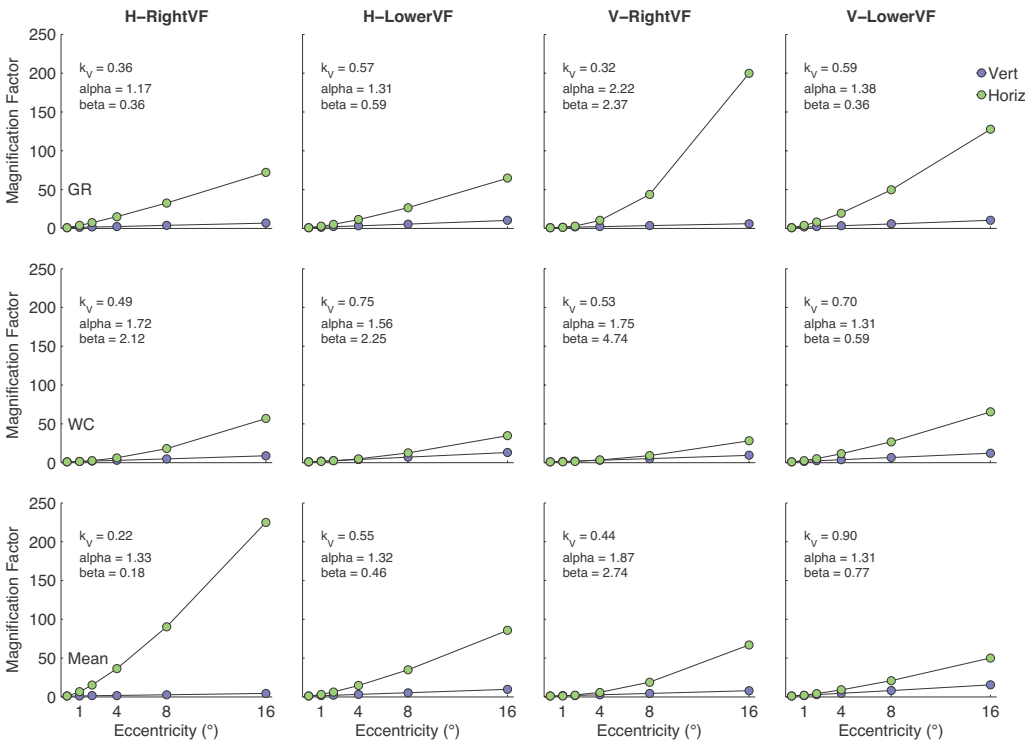

Figure 6. The horizontal and vertical magnification factors used in Figure 5 plotted as a function of eccentricity. Rows and columns are arranged as in Figures 2 to 5. Eccentricity in degrees visual angle is plotted on the x-axis and the rate of magnification is shown on the y-axis. The blue circles represent target size-at-threshold in the un-flanked conditions divided by target size-at-threshold at fixation (0°). The green circles represent sizes (and separations) for which size equals separation-at-threshold divided by the same quantity obtained at fixation. In each panel k_V represents the rate of the vertical shift while α and β together determine the rate of the horizontal shift that best characterizes the data.

The average r^2 value when eccentricity was included as a source of variability in the linear/nonlinear fit was .93 (see Table 1 for r^2 values by participant and by condition). The average r^2 value for the collapsed data was .65, which is even lower than that of the double scaling procedure ($r^2 = .71$) Refer to Table 2 for r^2 values for the scaled data by participant and by condition.

As with the double scaling method, the horizontal shift of the curves, as suggested by the values of α and β, results in an implausible prediction (Fig. 5). The smallest separation to size ratios predicted by the linear/nonlinear-scaling fits are in a range from .02 to .56. As with the linear fit these values are all less than 1 and therefore predict that target and flanker will overlap. See the preceding section (PG1) for details. Both the double linear and linear/nonlinear method (as per Poirier & Gurnsey, 2002) suggest that while a standard scaling procedure is adequate to scale isolated target stimuli across the visual field and compensate for visual under-sampling, they do not provide plausible accounts of crowding effects because the curves are shifted too far to the left, resulting in implausible $separation_E / size_E$ ratios.

Because the assumptions underlying the fits obtained with standard double scaling methods lead to untenable conclusions we must, for the moment, reject the conclusion that the curves at each eccentricity reflect different samples from the same underlying function. To address the implausibility of these fits we attempted three other analyses as per Gurnsey et al. (2011) to see if we could better characterize the data across the visual field.

Gurnsey et al., 2011: 'Raw' Scaling Method

In the previous two scaling methods (based on Poirier & Gurnsey, 2002) some of the size-versus-separation curves were shifted left of the point that would cause the target and flanker to overlap (Figs. 4 and 5). To deal with the implausibility of the two versions of the Poirier-Gurnsey method we first identified the point of maximum possible threshold elevation on each size-versus-separation curve, for each participant, in each condition, and at each eccentricity. This point would occur for target-flanker separations of 1x target size. Because we did not test separations of 1x target size we extrapolated from the existing data by fitting each curve in Figure 3 with a rectangular parabola. The grey dots associated with each curve in Figure 3 correspond to the point at which $\mu_E = separation_E / size_E = 1$.

A first step in this scaling method is to consider the limiting cases; i.e., the un-flanked thresholds and the smallest possible target-flanker separations. Figure 7 characterizes the horizontal and vertical shifts used to collapse the data from each panel of Figure 3 onto a single curve as shown in Figure 8. The blue circles in Figure 7 show un-flanked size thresholds at 1 to 16° relative to the un-flanked size thresholds at fixation; i.e., s_E / s_O. The green circles in Figure 7 show the points on the rectangular parabolas at 1 to 16° for which size-at-threshold (μ_{size}) = separation-at-threshold (μ_{sep}); *i.e.*, $\mu_{size} / \mu_{sep} = 1$. For clarification, the green circles in Figure 7 represent the sizes (or separations) corresponding to the grey dots in Figure 3 at eccentricities of 1 to 16° divided by the sizes (or separations) corresponding to the grey dots at fixation (0°); i.e., μ_E / μ_O. These limiting cases (s_E / s_O and μ_E / μ_O) show how the rectangular parabolas in Figure 3 shift up and to the right with eccentricity, respectively, within each panel.

The magnification factor (*MF*) is fit to the data as represented by the blue and green dots in Figure 3 by the function:

$$MF = 1 + kE \tag{16}$$

where k represents the rate of increase. It is clear that size-at-threshold in the un-flanked cases increases linearly with eccentricity. The magnification factors (y-axis, Fig. 7) represent the degree to which the functions shift up and to the right with eccentricity. The values of k_V represent the rate of the vertical shift and the values of k_H represent the rate of the horizontal shift. The proportion of variability (r^2) in the data is explained by the straight lines shown within each panel and the fits are quite good, explaining, on average, about 97% of the eccentricity-dependent variability in both s_E / s_O and μ_E / μ_O.

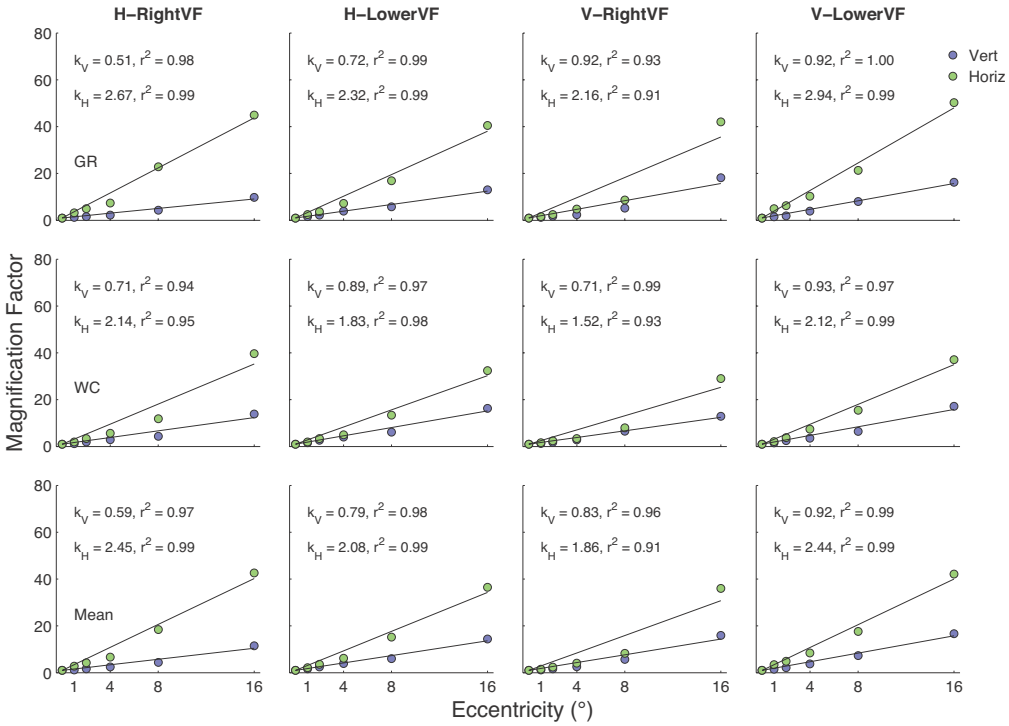

Figure 7. The horizontal and vertical magnification factors used in Figure 8 plotted as a function of eccentricity. Eccentricity in degrees visual angle is plotted on the x-axis and the rate of magnification is shown on the y-axis. The blue circles represent target size-at-threshold in the un-flanked conditions divided by target size-at-threshold at fixation (0º). The green circles represent sizes (and separations) for which size equals separation-at-threshold divided by the same quantity obtained at fixation. (These ratios show how the curves in Figure 3 shift rightwards with eccentricity, see results section for details). In each panel k_V represents the rate of the vertical shift and k_H represents the rate of the horizontal shift that best characterizes the data. The proportion of variability explained by these shifts is explained by r^2 and is described by the straight lines shown within each panel.

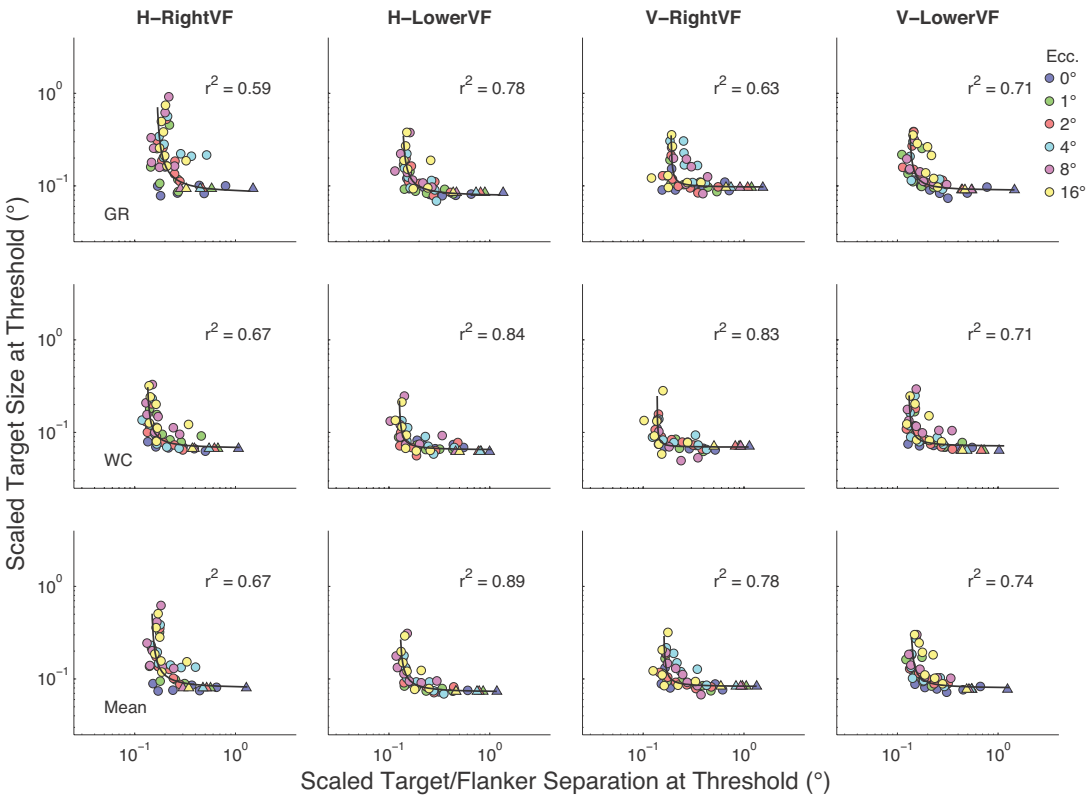

Figure 8. The scaled target size-at-threshold versus the scaled target-flanker separation-at-threshold. (See results section for details) Vertical and horizontal shifts were obtained by dividing the un-flanked target size threshold at each eccentricity by the un-flanked size threshold 0° eccentricity. Rows and columns are arranged as in Figures 2 to 7. Circles represent target-flanker separations of 1.25 to 8 times target size at each eccentricity. The continuous black line represents the best fitting rectangular parabola; see results section for details. The proportion of explained variability is given by r^2 in each panel.

The objective of this analysis was to shift data from all eccentricities onto a single curve to provide a concise characterization of the data. Because the present data set clearly requires a shift both leftward and downward we attempted three fitting methods to find the simplest characterization. The first method required the dividing the data points in Figure 3, separation-at-threshold, by μ_E / μ_O and the corresponding size-at-threshold by s_E / s_O. Then we determined the best fitting rectangular parabola to the scaled data. Figure 8 plots the shifted data along with the best-fitting rectangular parabola. Also shown is the proportion of variability that the parabola explains in the scaled data. The average r^2 value for the scaled data is 72% (Please note that our measure of fit is based on the diagonal distance from data point to curve in the log-log space shown as per Poirier and Gurnsey, 2002). The fit is better than the linear/nonlinear scaling method as per Poirier and Gurnsey (2002) at 65% and similar to the double scaling method (71%), but produces a plausible fit in which target and flanker are not predicted to overlap.

Gurnsey et al., 2011: Two linear scaling factors

The Gurnsey et al. (2011) 'Raw' scaling method produced an average r^2 value of .72, and more importantly, a plausible fit. However, we thought we might be able to provide a more concise characterization of the data if we replaced μ_E / μ_O with

$$M = 1 + k_H E \tag{17}$$

and s_E / s_O with

$$M = 1 + k_V E \tag{18}.$$

After scaling (shifting) the data in this way we once again found the best fitting rectangular parabola. However, these results explained only 53% of the variability in the

data on average (see Table 2 for r^2 values for the scaled data by participant and by condition). A far worse fit than when the data were scaled with μ_E / μ_O and s_E / s_O as in the Gurnsey et al. (2011) 'Raw' scaling method. Therefore, although the fits of $M = 1 + k_H E$ to μ_E / μ_O and $M = 1 + k_V E$ to s_E / s_O produce an average r^2 of about .97, there remains a large amount of residual variability about the rectangular parabola fit to the scaled data.

Gurnsey et al., 2011: Two nonlinear scaling factors

Finally, a third analysis was performed to see if a better fit could be achieved by replacing the linear magnification functions $M = 1 + k_H E$ and $M = 1 + k_V E$ with non-linear magnification functions,

$$M = 1 + E^{\alpha_H} / \beta_H \tag{19}$$

and

$$M = 1 + E^{\alpha_V} / \beta_V \tag{20}.$$

The preceding section "Poirier & Gurnsey (2002): Linear/Nonlinear Scaling Method" provides details on the parameters α and β. Although these results explained 63% of the variability in the data they remain substantially worse than the results of the original Gurnsey et al. (2011) scaled 'Raw fits' which explained 72% of the variability (see Table 2 for r^2 values for the scaled data by participant and by condition). Therefore, the fits of $M = 1 + E^{\alpha_H} / \beta_H$ to μ_E / μ_O and $M = 1 + E^{\alpha_V} / \beta_V$ to s_E / s_O are again very good (r^2 = .97) but there remains a large amount of residual variability about the rectangular parabola fit to the scaled data.

The Shape of the Interference Zones.

The four conditions of the experiment - Visual Field, Flanker Orientation, Eccentricity and Relative Separation - were chosen to examine the interaction of flankers and meridian. Figure 9 summarizes the main result of this analysis. The threshold ratios in the parallel and perpendicular flanker-to-target conditions in the right visual field (left panel) and lower visual field (right panel) are plotted as a function of relative target-flanker separation. The data have been averaged across participants. We divided each data point S by the corresponding data point from the alternate configuration in the same visual field,

$$s_{E_{THR}} \text{ (H-RVF)} / s_{E_{THR}} \text{ (V-RVF)} \quad (21a)$$

and conversely,

$$s_{E_{THR}} \text{ (V-RVF)} / s_{E_{THR}} \text{ (H-RVF)} \quad (21b),$$

where $s_{E_{THR}}$ is target size-at-threshold averaged across participants for a given configuration in either the right or lower visual field. In almost all cases the ratios exceed 1. This means that in the case of the right visual field (left panel) there is a stronger crowding effect (increased target size thresholds) when flankers are arranged horizontally about the target and in the case of the lower visual field (right panel) the effect is strongest when flankers are arranged vertically about the target. Our results are consistent with the notion that interference zones are elliptical in shape and oriented towards the fovea (Pelli et al., 2004; Toet & Levi, 1992).

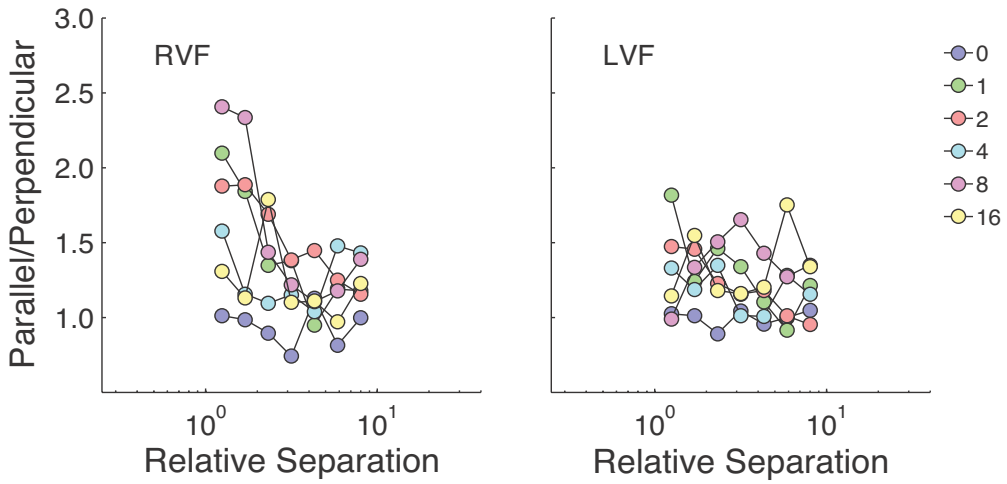

Figure 9. The effect of target-flanker configuration in the RightVF and LowerVF. The ratio of size threshold for parallel flankers to perpendicular flankers is shown as a function of relative separation for the RightVF (left panel) and the LowerVF (right panel). The ratios have been formed from the average data (Row 3) of Figure 2.

Discussion

The present study extends what is known about task differences from the crowding literature, and sensitivity to symmetry from the symmetry literature, by showing that symmetrical targets are susceptible to interference from flanking items across the visual field. Using the method outlined by Gurnsey et al. (2011), the present study explored issues similar to those often debated in the crowding literature. Our first question examined the effect of crowding at fixation for which there was no evidence at the five largest target-flanker separations (Figs. 2 and 3). However, there is some evidence of crowding at the smallest two relative separations (1.25, 1.70 times target size). This represents a percentage increase over the un-flanked condition of between 27 and 72% at fixation (0º) for participant GR and between 56 and 86% for participant WC across the four conditions. This is consistent with previous findings showing modest spatial interactions at fixation extending over a small range of target-flanker separations (Gurnsey et al., 2011; Latham & Whitaker, 1996; Liu & Ariditi, 2000; Pelli et al., 2007; Toet & Levi, 1992).

It was also proposed that the magnitude of spatial interference in the peripheral visual field would increase and that double linear magnification may not be sufficient to characterize performance across the visual field. At most eccentricities the upper portion of the size-versus-separation curves become almost parallel to the y-axis therefore at some point critical separation-at-threshold becomes independent of target size (Fig. 3). At 16º (yellow circles) the effect is pronounced and threshold elevations over the un-flanked condition are far greater at 16º (for GR: 291 to 697% and for WC: 243 to 377%) than at 0º. Because the magnitude of the crowding effect did, in fact, increase with eccentricity

standard linear double-scaling procedures provide inappropriate characterizations of the data.

To relate the extent of crowding to increasing eccentricity, a nonlinear vertical shift was attempted to collapse the data back to the foveal standard (see Poirier and Gurnsey (2002): Linear/nonlinear Scaling method, Fig. 5). However, this fit explained less variability ($r^2 = .65$) than the double linear fit ($r^2 = .71$). This is an interesting discovery given that the linear/nonlinear fit had a greater number of parameters.

Both of these scaling methods yield implausible results. The best fitting functions predict stimulus configurations at fixation (0º, blue circles, Fig. 4) that violate the assumption that crowding effects only exist for $separation_E / size_E$ ratios of 1 or greater. Otherwise any observed effect may be attributed to masking. To address the implausibility of the fit the point of maximum possible threshold elevation was identified (target-flanker separations = 1x target size). This method produced a better fit ($r^2 = .72$, 'Raw') than the previous nonlinear fit ($r^2 = .65$, PG2) and roughly the same amount of explained variability as the double linear fit ($r^2 = .71$, PG1). However, this method eliminates the prediction that targets and flankers will overlap and therefore provides a tenable fit.

We attempted two other scaling procedures in an effort to provide a more concise characterization of the data. The first employed two linear scaling factors but only 55% of the variability in the data on average was explained by this result (Table 2, method LL). The second employed two nonlinear scaling factors (Table 2, method NLNL). The average r^2 for this fit is .63. Although, the fits of the scaling factors to the limiting cases

(μ_E / μ_O and s_E / s_O) consistently produced an r^2 value of $\approx .97$ a large amount of residual variability about the rectangular parabola fit to the scaled data remained.

The Gurnsey et al. (2011) 'Raw' scaling method produced the best characterization of the data ($r^2 = .72$) that is plausible given the assumptions of the crowding phenomenon. The k_V values range from .51 to .93, with a mean $\bar{k}_V$ of .79 (SEM = .053). We find our estimate of $\bar{k}_V = .79$, to reflect eccentricity dependant changes in un-flanked size thresholds, is in rough agreement with previous studies on symmetry perception (Gurnsey et al., 1998a; Saarinen, 1988; Sally & Gurnsey, 2001). Figure 7 revealed that sensitivity to a flanked target decreases at a much greater rate than resolution of an isolated one. These results are consistent with previous studies that have separated the two factors (Gurnsey et al., 2011; Latham & Whitaker, 1996; Toet & Levi, 1992) and not dissimilar to previous reported average values such as $k_V = 1.21$ (Barrett et al., 1999), $k_V = 1.29$ (Saarinen, 1988) or $k_V = .88$ (Sally & Gurnsey, 2001).

In the present study we have employed the methodology used by Gurnsey et al. (2011) to study crowding effects for letter identification, and grating and 'T' orientation discrimination tasks. As in Gurnsey et al. the growth of interference regions with eccentricity (the horizontal shifts of the curves in Figure 3; green symbols in Figure 4) is much faster than the loss of resolution with eccentricity (the vertical shifts of the curves in Figure 3; blue symbols in Figure 4). Gurnsey et al. (2011) also found that the horizontal shift equating the threshold levels, across the visual field, of three separate tasks that used alphanumeric stimuli (letter identification, and grating [ ] and 'T' [

⊤ ⊢ ⊥ ⊣] orientation discrimination) increased non-linearly with eccentricity (we continue this comparison in the General Discussion).

Finally we examined the possibility of an anisotropy as a function of stimulus configuration within the present results. Figure 9 shows that in both cases target size-at-threshold is higher when targets are flanked vertically rather than horizontally in the lower visual field and horizontally rather than vertically in the right visual field, consistent with the view that crowding zones are elliptical and oriented to the fovea (Pelli et al., 2004; Toet & Levi, 2002). Although we found no evidence of an anisotropy in visual field meridian at 0º, it is possible that there is a modest anisotropy with regard to visual field meridian and the crowding effect for the data at 16º. (We will return to this point in the General Discussion.)

The consistent result throughout the five analyses presented in Experiment 1 is that sensitivity to a crowded symmetrical target drops off at a far quicker rate across the visual field than does resolution of an isolated symmetrical target. This is in accord with other studies that have separated these two factors (Gurnsey et al., 1998a; Latham & Whitaker, 1996).

Introduction-Experiment 2a

There is increasing evidence that the properties of flankers determine the degree to which they will interfere with target perception. Properties such as flanker pattern orientation (Levi & Carney, 2009; Livne & Sagi, 2010; Poder & Wagemans, 2007), grouping and configuration around the target (Levi & Carney, 2009; Livne & Sagi, 2010), number (Levi & Carney, 2009; Poder & Wagemans, 2007), spacing (Saarela, Sayim, Westheimer, & Herzog, 2009; Saarela, Westheimer, & Herzog, 2010) and similarity to target (Levi & Carney, 2009; Livne & Sagi, 2010; Poder & Wagemans, 2007) all play a role in determining the extent of interference between target and flankers. As previously noted, the positioning of the flankers with respect to the target is an important factor in crowding studies because there is evidence that the regions of interference are elliptical in shape and oriented towards the fovea (Experiment 1-Fig. 9; Pelli et al., 2007; Toet & Levi, 1992 and others). We also noted an orientation bias favouring vertical symmetry in several reports (e.g., Barlow & Reeves, 1979; Jenkins, 1985). Given these two orientation factors, we looked at how global stimulus configuration (flanker positioning) and orientation contrast between symmetrical targets and symmetrical flankers might interact to affect the results in a task requiring detection of symmetrical stimuli.

A number of studies have used grating stimuli to look at how the relative orientations of targets and flankers affect target identification or discrimination (Levi & Carney, 2009; Poder & Wagemans, 2007; Poder, 2008). For example, there is evidence to suggest that flankers are less disruptive if their orientation differs from that of the target

by 45º and more so at 90º (Levi & Carney, 2009; Livne & Sagi, 2010). There is also evidence that a possible pooling in the visual system of the orientation signals from the flankers may affect the perception of the central target (Parkes et al., 2001; Poder & Wagemans, 2007).

Poder and Wagemans (2007) examined orientation discrimination of a central Gabor, presented at 4º eccentricity surrounded by two, four or six flankers. They found that the rate of 'vertical' responses increased in *almost* linear fashion as the number of vertical flankers increased, irrespective of target orientation. This is consistent with the well-known study by Parkes, Lund, Angelucci, Solomon and Morgan (2001) that showed a pooling effect in a crowding task requiring participants to discriminate the orientation of a target Gabor patch surrounded by flanker patches of random orientation. It seems that flankers do not simply mask the target. Rather, they encourage percepts that are inaccurate combinations of targets and flankers.

There are crowding studies that have included an analysis of configuration, i.e., a horizontal versus a vertical arrangement of flankers, and have found an anisotropy with regard to visual field. Quite simply, these studies find that in the lower visual field the zone of interference is considerably larger when flankers are oriented above and below the target, as opposed to left and right (Pelli et al., 2007; Levi, 2008; Toet & Levi, 1992).

In Experiment 2a participants were asked to discriminate horizontal and vertical symmetry from random patches in a 2AFC discrimination task. Testing was always done in the lower visual field at 8º eccentricity. Flankers could be of horizontal or vertical orientation and placed above and below or left and right of the target. Based on the literature just reviewed we suggest that: (a) Flankers placed above and below the target

should be more effective than those placed left and right because of the shapes of the interference zones (consistent with Exp. 1 of this paper-Fig. 9; Pelli et al., 2007; Toet and Levi, 1992). (b) Flankers should be more effective when they have the same orientation as the target (Levi & Carney, 2009; Poder & Wagemans, 2007). (c) Flankers should be least effective when they have an orientation 90º to the target (Levi & Carney, 2009). (d) Flankers will have less of an effect on vertical targets than horizontal targets overall. Although the crowding literature has no example from which to draw, the symmetry literature shows a strong vertical bias (e.g., Barlow & Reeves, 1979; Jenkins, 1985).

Method-Experiment 2a

Participants

The same two subjects from Experiment 1 participated in Experiment 2a.

Apparatus

All aspects of stimulus generation, presentation and data collection were the same as in Experiment 1.

Stimuli

The stimuli were 7 x 7 arrays of black and white checks. Pixel size was approximately .188 mm. Targets were symmetrical about the horizontal or vertical axis, or a random patch. Flankers were symmetrical around the horizontal or vertical axis. Figures 10 and 11 provide an illustration of the target-flanker configurations and pattern orientations. Targets could be flanked horizontally (flankers to the left and right of the target) or vertically (flankers above and below the target) with a centre-to-centre separation of 1.00, 1.41, 2.00, 2.83, 4.00, 5.66, 8.00 times target size. Targets were also presented in an un-flanked condition. The stimulus was presented 8º below fixation in the lower (LowerVF) visual field, on the vertical midline. As before, the stimuli were always centred on the screen and eccentricity was controlled by the position of the fixation dot. Viewing distance was 40 cm to maximize the number of pixels per check. Luminance and contrast were the same as in Experiment 1.

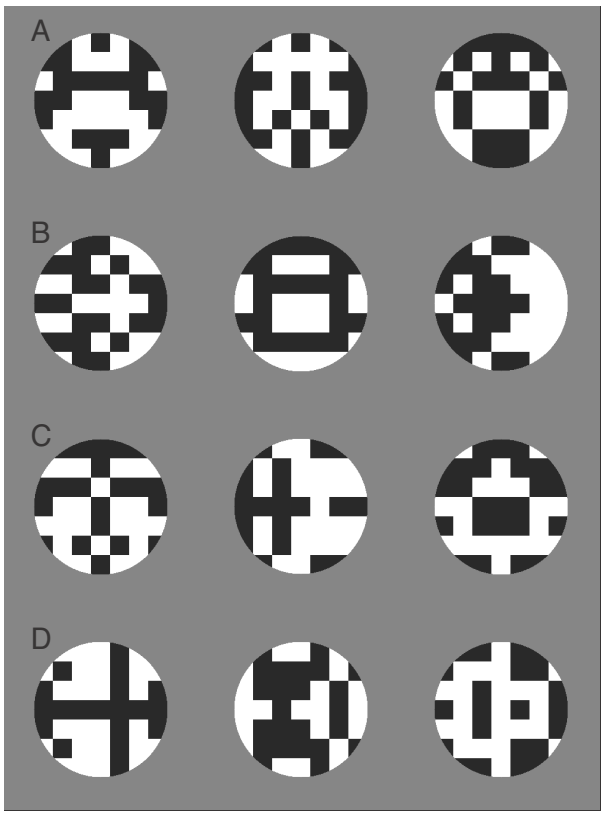

Figure 10. The stimuli for Experiment 2a and b in the horizontal configuration as presented at 8º in the LowerVF. Each row represents an example taken from each local pattern condition. In Row A both targets and flankers are vertical, in Row B targets are vertical and flankers are horizontal, in Row C targets are horizontal and flankers are vertical and in Row D both targets and flankers are horizontal. This represents a subset of possible patterns.

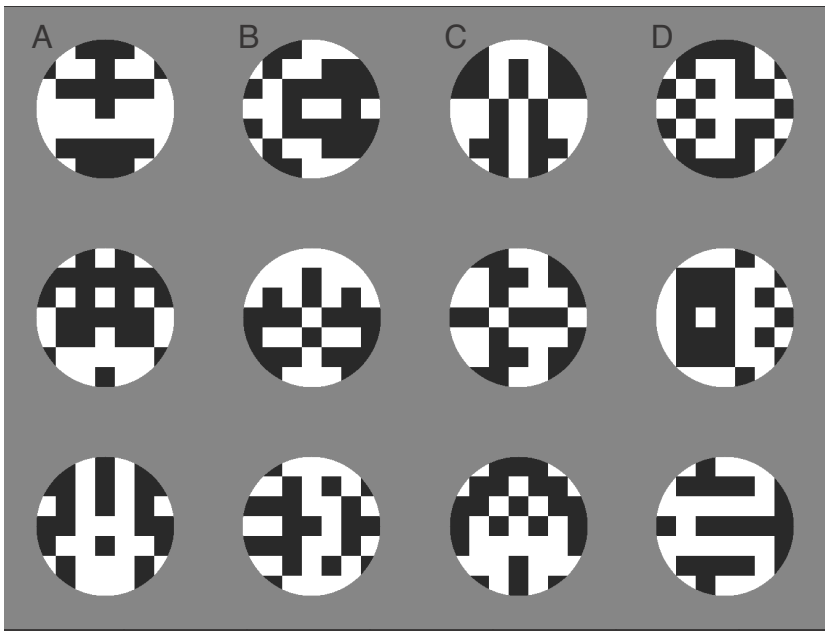

Figure 11. The stimuli for Experiment 2a and b in the vertical configuration as presented at 8º in the LowerVF. Each column represents an example taken from each local pattern condition. In Column A both targets and flankers are vertical, in Column B targets are vertical and flankers are horizontal, in Column C targets are horizontal and flankers are vertical and in Column D both targets and flankers are horizontal. This represents a subset of possible patterns.

Procedure

On each trial of the experiment the participants' task was to report whether the target patch was symmetrical or random. The target was flanked by two symmetrical flankers at one of the 7 relative separations (1.00, 1.41, 2.00, 2.83, 4.00, 5.66, 8.00, and ∞ times target size or the un-flanked condition). A Quest adaptive procedure (Watson & Pelli, 1983) adjusted size of the entire stimulus (target + flankers) on the basis of the participant's response history; stimulus size was decreased during periods of correct responses and increased during periods of incorrect responses. The goal of the adaptive procedure was to find the target size that elicited 81% correct in the two-alternative forced choice task (2AFC). The adaptive procedure ran until this goal was achieved or 100 trials, which ever came first.

A small green fixation dot was placed either above (for the lower visual field) or to the left (for the right visual field) of the stimulus. The stimulus was presented for approximately 333 ms, after which the participant entered his or her response on the number keypad, a *1* for a symmetrical stimulus and a *2* for a random patch. Incorrect responses were signalled by a 300 ms, 400 Hz tone.

There were four factors in the experiment: Configuration of Flankers (horizontal or vertical), Target Orientation (horizontal or vertical), Flanker Orientation (horizontal or vertical, see Figs. 10 and 11) and Relative Separation (1.00, 1.41, 2.00, 2.83, 4.00, 5.66, 8.00, and ∞ times target size). For each of these 64 conditions we obtained and averaged four target size thresholds for the horizontal configuration and three for the vertical configuration. The conditions were not interleaved. Each block contained only one condition at a time. For example participants were presented with a horizontally aligned

trigram at all separations for one target-flanker pattern orientation combination, before proceeding to the next condition. Prior to data collection participants received sufficient practice to become familiar with the task. As in Experiment 1, testing started with the un-flanked condition and progressed though the smaller relative separations.

Results-Experiment 2a

The Effect of Target Orientation

Figure 12 plots the effect of target pattern orientation for two participants in the lower visual field as a function of target-flanker separation on a log-log scale. The y-axis represents target size-at-threshold and the x-axis represents the range of relative target-flanker separations (1.00, 1.41, 2.00, 2.83, 4.00, 5.66, 8.00, and ∞ times target size). Relative separation has been plotted here because of noise in the data set. We have represented the data this way as depicting absolute separation magnifies the differences and makes the data harder to interpret. The data can be compared to that of Figure 2 in Experiment 1 at 8º (purple circles). As target size-at-threshold decreases relative target-flanker separation increases. The individual data are plotted in Rows 1 (participant GR) and 2 (participant WC) and the average values are plotted in Row 3. The data points represent target size-at-threshold for the horizontal target (blue circles) and the vertical target (green circles). The un-flanked condition is represented by triangles. Columns 1 and 2 depict horizontal and vertical flankers in the horizontal configuration (HF/HC and VF/HC); Columns 3 and 4 depict horizontal and vertical flankers in the vertical configuration (HF/VC and VF/VC).

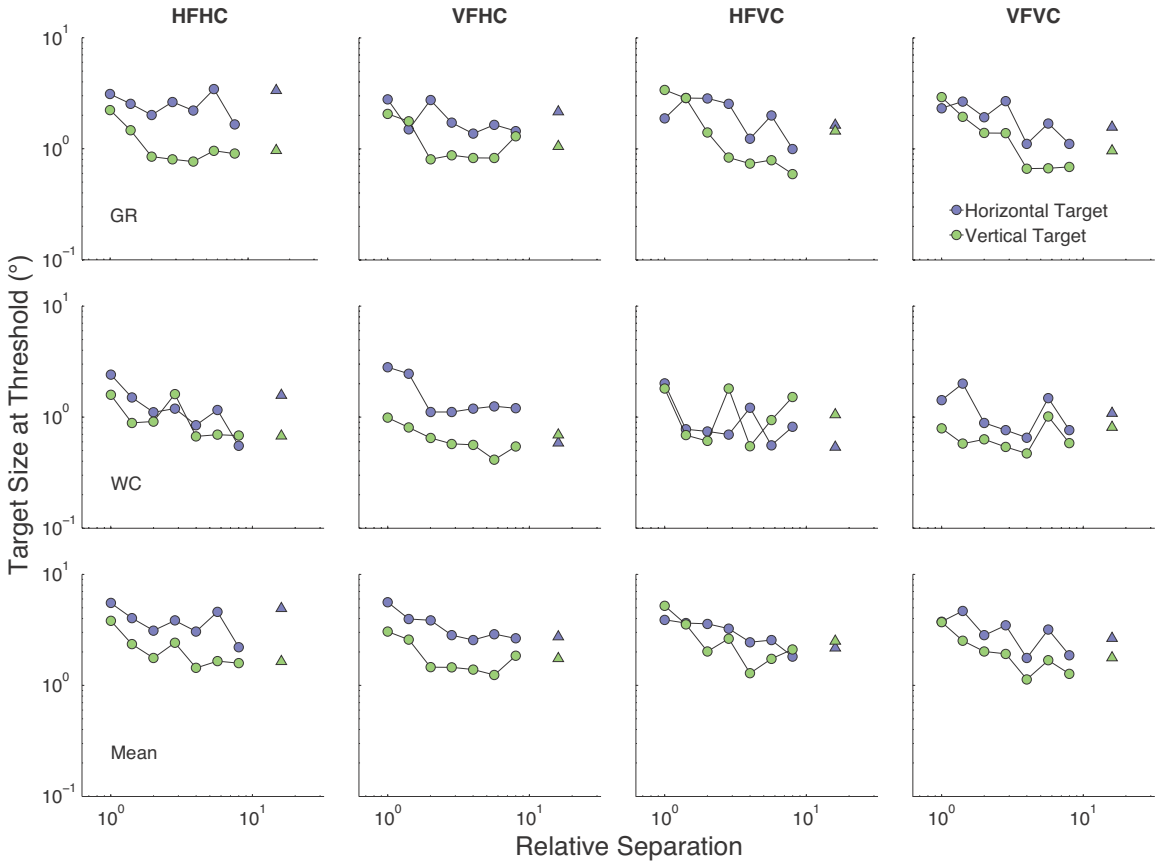

Figure 12. Experiment 2a: The Effect of Target Orientation. The effect of target orientation for two participants in the lower visual field plotted as a function of relative target-flanker separation on a log-log scale. Rows represent participants, GR, WC and the averaged data respectively. The data points are represented as target size-at-threshold for the horizontal target (blue circles) and the vertical target (green circles). Triangles represent the un-flanked condition. Columns 1 and 2 represent horizontal and vertical flankers in the horizontal configuration (HF/HC and VF/HC). Columns 3 and 4 represent horizontal and vertical flankers in the vertical configuration (HF/VC and VF/VC).

There was a trend for thresholds to be higher for horizontal targets than for vertical targets but this difference was more frequently present for GR than WC. GR also produced steeper threshold decreases in the vertical configuration regardless of target or flanker orientation. WC showed almost no difference in threshold values between the two target orientations with the exception of horizontal targets surrounded by vertical flankers in the horizontal configuration.

Figure 13 summarizes the interaction of targets, flankers and configuration averaged over relative separation. The y-axis depicts the mean of all size thresholds for a given condition. In other words, it represents a collapsing of all target-flanker separations. The left panel represents the horizontal configuration and the right panel, the vertical configuration. Each pair of bars represents horizontal flankers (blue) and vertical flankers (green). The left pair of bars in each panel corresponds to the data obtained with horizontal targets and the right pair to vertical targets. The error bars represent 1 standard error of the mean.

On average the horizontal targets produced higher size thresholds than the vertical targets. In the vertical configuration the performance with the horizontal target produces the lowest thresholds as well, although the discrepancy is not as great. The horizontal configuration produces both the highest thresholds for horizontal targets (surrounded by horizontal flankers) and the lowest thresholds for vertical targets (surrounded by vertical flankers).

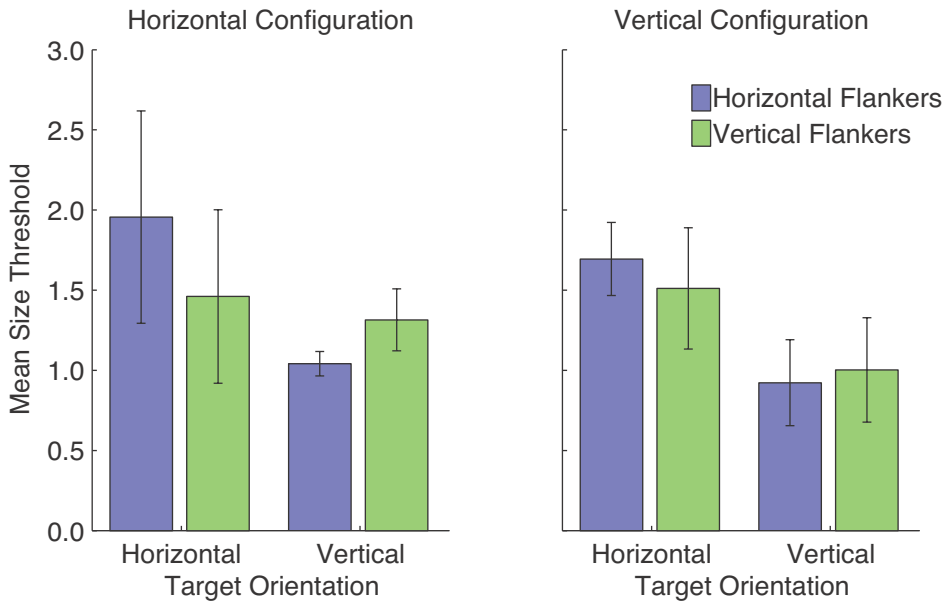

Figure 13. The Main Effect of Target Orientation. Each panel represents a configuration (vertical, horizontal), each pair of bars represents flanker orientation (horizontal flankers, vertical flankers, repeated twice in each panel) the left pair of bars in each panel represents the horizontal targets and the right pair the vertical targets. The data is averaged over the two participants. The y-axis represents the mean size threshold for each condition. The error bars represent 1 standard error of the mean.

The Effect of Stimulus Configuration

Figure 14 plots the effect of stimulus configuration for the two participants in the lower visual field as a function of target-flanker separation on a log-log scale. The arrangement of rows, the designation of the x- and y-axes, and the data point assignments are the same as in Figure 12. The blue circles represent the horizontal configuration and the green circles represent the vertical configuration. Columns 1 and 2 represent horizontal targets surrounded by horizontal flankers and vertical flankers respectively (HF/HT and VF/HT). Columns 3 and 4 represent vertical targets surrounded by horizontal and vertical flankers respectively (HF/VT and VF/VT). There seems to be no effect of stimulus configuration for either participant. This result stands in contrast to the results found in Experiment 1 (Fig. 9) and other studies (Pelli et al., 2004; Toet and Levi, 1992). Both participants show the regular pattern of decreasing sensitivity with increasing target-flanker separation regardless of a horizontal or vertical configuration of flankers around the target.

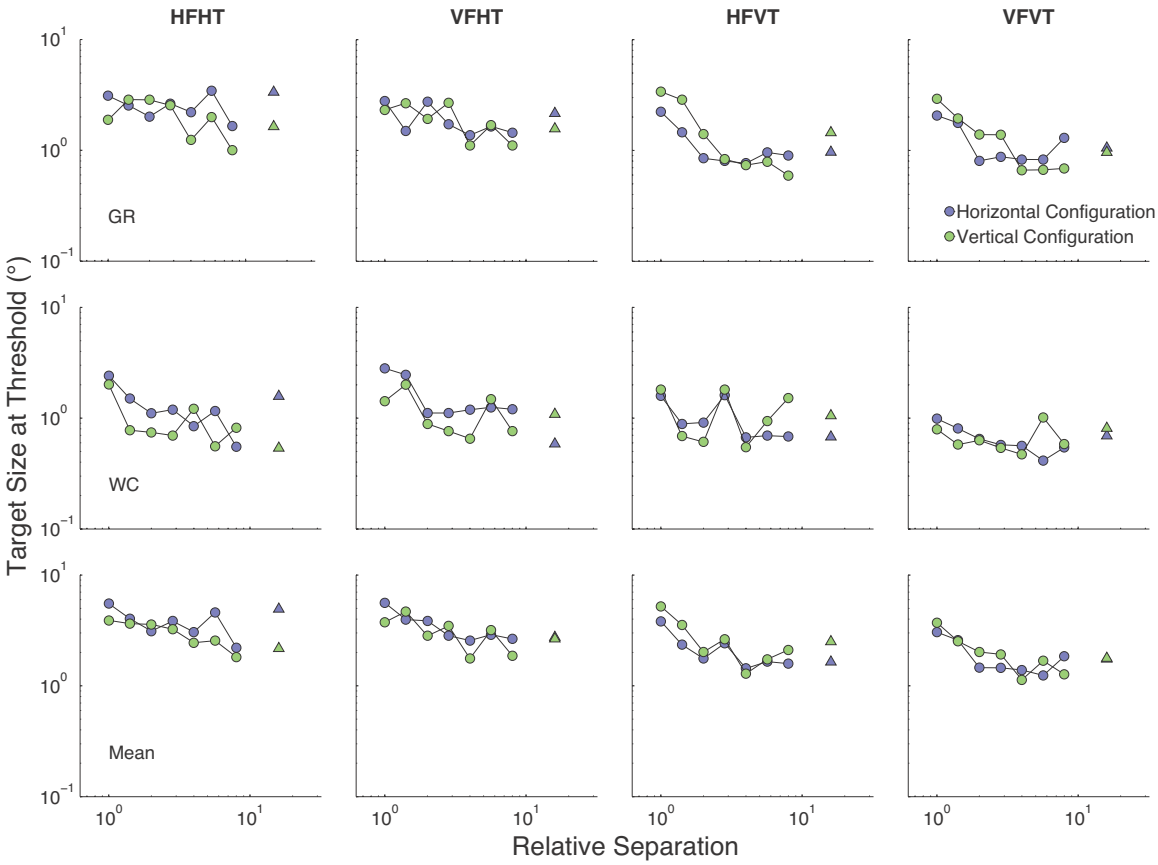

Figure 14. Experiment 2a: The Effect of Configuration. The effect of configuration for two participants in the lower visual field plotted as a function of relative target-flanker separation on a log-log scale. The arrangement of rows, the designation of the x- and y-axes and the data point assignments are the same as in Figure 12. Columns 1 and 2 represent horizontal targets surrounded by horizontal flankers (HF/HT) and vertical flankers (VF/HT). Columns 3 and 4 represent vertical targets surrounded by horizontal flankers (HF/VT) and vertical flankers (VF/VT).

The Effect of Flanker Orientation

Figure 15 plots the effect of flanker pattern orientation for two participants in the LowerVF as a function of target-flanker separation on a log-log scale. The graph follows the form of Figures 12 and 14. Blue circles represent horizontal flanker pattern orientation and green circles represent the vertical orientation. Columns 1 and 2 depict horizontal or vertical targets in the horizontal configuration (HT/HC and VT/HC) and Columns 3 and 4 depict horizontal and vertical targets in the vertical configuration (HT/VC and VT/VC).

There is no effect of flanker orientation on the discrimination of either a vertical target or a horizontal target in either configuration. WC (Row 2) produced very noisy data for the vertical targets surrounded by horizontal flankers in the vertical configuration. For the same condition the data produced by GR are cleaner and there is a very steep threshold decrease for vertical targets in a vertical configuration regardless of flanker orientation. However, the data remain inconsistent with the notion that crowding effects can be modulated by the relative orientation differences between target and flankers (Levi & Carney, 2009).

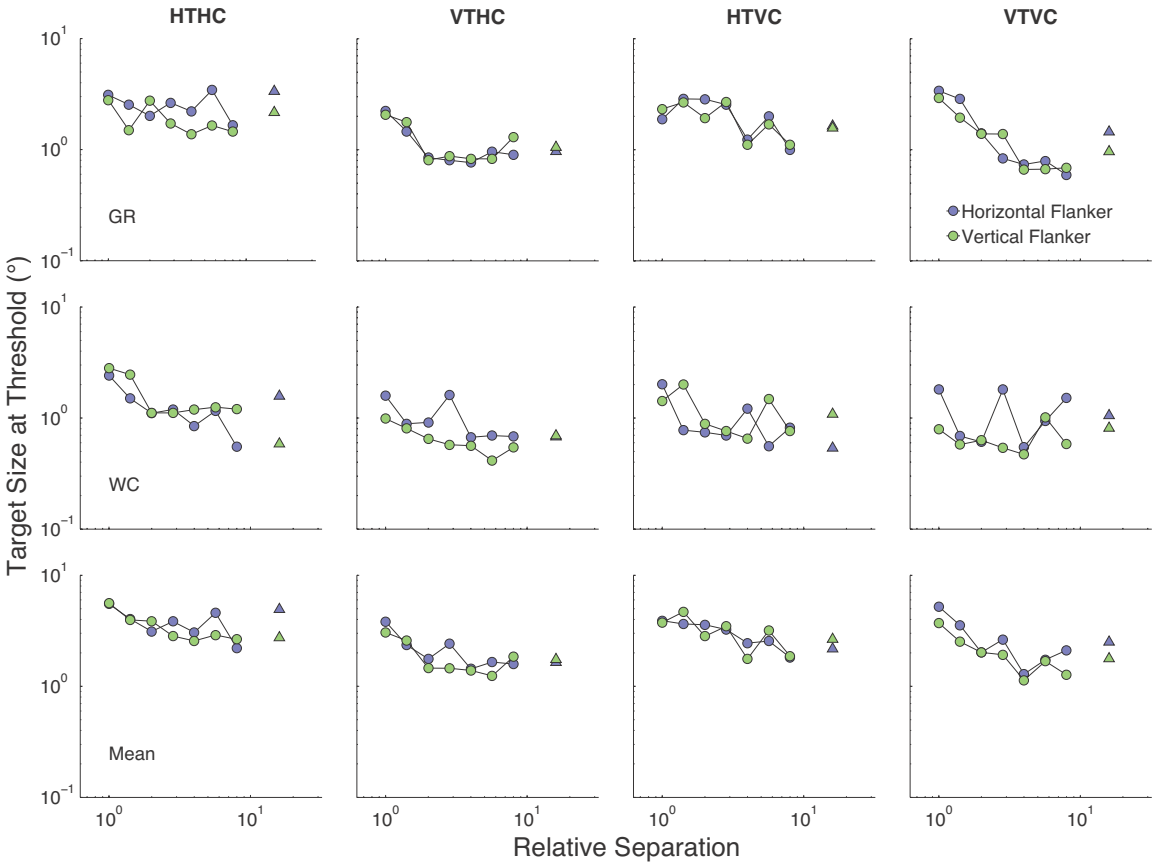

Figure 15. Experiment 2a: The Effect of Flanker Orientation. The effect of flanker orientation for two participants in the lower visual field plotted as a function of relative target-flanker separation on a log-log scale. The graph follows the same form as Figures 12 and 14. Columns 1 and 2 represent horizontal targets flanked horizontally or vertically (HT/HC and HT/VC) and Columns 3 and 4 represent vertical targets flanked horizontally or vertically (VT/HC and VT/VC).

Discussion-Experiment 2a

In Experiment 2a participants were asked to discriminate horizontal or vertical symmetry from a random patch in a 2AFC discrimination task at 8º in the LowerVF. The objective was to examine the properties of the flankers themselves that may contribute to their interference with the target. In all conditions threshold values decreased as target-flanker spacing increased (Figs. 12, 14 and 15). This is similar to the pattern found in Experiment 1 (see Fig. 2, 8º, purple circles) and suggests stimuli behave in a similar manner to alphanumeric or grating type stimuli in a crowding paradigm, at least at 8º eccentricity (Gurnsey et al., 2011). However, threshold elevation was the same regardless of stimulus configuration (Fig. 14) or flanker orientation (Fig.15). This is interesting as we found consistent configuration effects in Experiment 1 of this paper.

There was no effect of relative flanker and target orientation. This is contrary to evidence that when flankers and targets are most similar, as when vertical targets are surrounded by vertical flankers, for example, targets are harder to discriminate (Levi & Carney, 2009; Livne & Sagi, 2010; Poder & Wagemans, 2007). It also runs contrary to the notion that crowding is reduced when flankers and targets differ in their relative orientation by 90º (Levi & Carney, 2009).

Surprisingly, the data did reveal a modest effect of target orientation (Fig. 12). Regardless of flanker orientation or configuration; horizontal targets were the harder of the two to discriminate (Fig. 13). The above result requires a caveat however as an inspection of the raw data revealed that the effect was largely for participant GR (Fig. 12). This may have inflated horizontal target size thresholds, especially with only two participants. The error bars in Figure 13 also overlap across conditions as a result of the

inherent subject variability discussed previously. With this in mind these results can be considered consistent with a large literature that has found an increased sensitivity to symmetrical targets with a vertical axis of orientation across the visual field (Barlow & Reeves, 1979; Jenkins, 1985).

As previously mentioned some participants might have had difficulty with the stochastic nature of the stimuli. The method used prevented a template matching strategy, however, it also means that two nominally identical stimuli (e.g., stimuli of identical size) might differ in 'perceptual salience', making it difficult to reliably estimate a threshold using the Quest method (see the Methods section of Experiments 1 and 2a. Figures 10 and 11 display example stimulus patterns.). To see if it was possible to smooth out the raw participant data and eliminate the need to converge on a target threshold size we attempted to replicate a subset of the conditions in Experiment 2a using the Method of Constant Stimuli.

Introduction-Experiment 2b

Experiment 2a found that the only consistent effect on target size thresholds was the orientation of the target. Overall, the horizontal target produced higher thresholds regardless of the other factors. However, the raw data was quite noisy. Experiment 2b attempts to replicate a subset of the conditions from Experiment 2a using the Method of Constant Stimuli. In this way we can compute a percentage correct for each stimulus size from which to calculate target size-at-threshold (Exp. 2b, results section). We hoped to eliminate a portion of the variability using this method. For Experiment 2b we elected to test only the vertical target orientation at 8º eccentricity in the lower visual field. Because the data of Experiment 2a are somewhat noisy it seems prudent to study the most salient symmetrical target orientation as a further effort to smooth the data for consideration of this alternate method.

In Experiment 2b participants were asked to distinguish the presence of vertical symmetry from random noise in a 2AFC discrimination task. Testing was always done in the lower visual field at 8º eccentricity. Flankers could be of horizontal or vertical orientation and placed above and below or left and right of the target. The predictions are the same as those made in Experiment 2a. Firstly, flankers organized in a configuration following the predicted pattern of interference across the visual field will have the greatest effect (consistent with Experiment 1-Fig. 9; Pelli et al., 2004; Toet and Levi, 1992). Secondly, flankers should be more effective when they have the same orientation as the target (Poder & Wagemans 2007; Levi & Carney, 2009) and least effective when they have an orientation 90º to the target (Levi & Carney, 2009).

Method-Experiment 2b

Participants

The same two subjects from Experiment 1 and Experiment 2a participated in Experiment 2b.

Apparatus

All aspects of stimulus generation, presentation and data collection were the same as in Experiment 1 and 2a.

Stimuli

The stimuli were 7 x 7 arrays of black and white checks. Target arrays were either symmetrical about the vertical axis or random patches. Flankers could be of either horizontal or vertical orientation. As in Experiment 1 and 2a targets could be flanked horizontally (flankers to the left and right of the target, Fig. 10) or vertically (flankers above and below the target, Fig. 11). Table 3 provides the seven sizes presented for each of the 7 relative, centre-to-centre separations. These configurations were presented at 8º in the lower (LowerVF) visual field on the vertical midline at viewing distances of 40 cm. The target centre was always presented in the centre of the screen. Luminance and contrast were the same as in Experiments 1 and 2a.

Procedure

Participants were asked to discriminate between a random and symmetrical target patch in a 2AFC task. Two symmetrical flankers surrounded the target at each of the 7 relative separations. The Method of Constant Stimuli was used to determine the level of

accuracy. The goal of the procedure was to find the target size that elicited 81.6% correct in the 2AFC.

A small green fixation dot was placed above the stimulus. The stimulus was presented for approximately 333 ms, after which the subject entered his or her response, a 1 for a present symmetrical stimulus and a 2 for a random patch. Incorrect responses were signalled by a 300 ms, 400 Hz tone.

There were three factors in the experiment: Configuration of Flankers (horizontal or vertical), Flanker Orientation (horizontal or vertical, Figs. 10 and 11) and Relative Separation. For each of the 32 conditions, participants were presented with two blocks of twenty-five replications for each of the seven stimulus sizes. As previously mentioned the target pattern was either vertically oriented or random. The two blocks of trials were averaged for each participant. The sizes were not interleaved and were presented from smallest to largest within each block. The conditions were also not interleaved, such that each block contained only one condition at a time. For example, a participant would respond to presentations of a vertical target surrounded by vertical flankers in a horizontally configured trigram at all size and separations before proceeding to the next condition. Prior to data collection subjects received sufficient practice to become familiar with the task.

Results-Experiment 2b

The Effect of Flanker Orientation-2b

Figure 16 plots the effect of configuration for two participants in the lower visual field as a function of target-flanker separation on a log-log scale. Target size-at-threshold is plotted along the y-axis and target-flanker separation on the x-axis. To calculate target

size-at-threshold from percent correct (as depicted in Figures 16 and 17) we first fit the psychometric curve with a Weibell Function (a sigmoidal cumulative density function) normalized to a range from .5 to 1. We were then able to determine the target size that elicited 81.6% correct in the 2AFC task.

The three rows from top to bottom represent values for GR, WC and the averaged results. The left column represents vertical targets surrounded by either vertical or horizontal flankers in the horizontal configuration (blue circles). The right column depicts the same two conditions in the vertical configuration (green circles). Size-at-threshold is plotted along the y-axis and target-flanker separation is plotted on the x-axis. For both participants overall target size-at-threshold decreases as target size and target-flanker separation increases. There was very little evidence of a flanker orientation effect.

The Effect of Stimulus Configuration-2b

Figure 17 plots the effect of configuration for two participants in the lower visual field as a function of target-flanker separation on a log-log scale. The arrangement of rows is the same as in Figure 16. The conditions in the left and right columns are vertical targets surrounded by vertical flankers and horizontal flankers respectively. Data points are represented as blue and green circles for the vertical and horizontal configurations, respectively. As before target size-at-threshold decreases as target size and target-flanker separation increases.

There is a trend of interest in this data set. It seems that vertical flankers are more effective than horizontal ones in the vertical configuration consistent with Poder and Wagemans (2007) and Levi and Carney (2009) and the notion that similar flankers are most effective. Conversely horizontal flankers are more effective than vertical ones in the

horizontal configuration consistent with Levi and Carney (2009) and the notion that flankers 90º relative to the target are least effective. We have not quantified this observation however as the trend is modest, and we have tested only with vertical targets at 8º eccentricity.

Overall the data in Experiment 2b are much cleaner than those of Experiment 2a. The fits were quite good for the averaged data and the explained variability given by r^2 for the horizontal configuration produced values of .96 and .87 for horizontal and vertical flanker conditions respectively and .94 and .96 for the horizontal and vertical flanker conditions in the vertical configuration.

Discussion-Experiment 2b

Experiment 2b used the Method of Constant Stimuli to revisit the issue of stimulus configuration and flanker orientation. The raw participant data were noticeably cleaner with this method than in Experiment 2a for the same conditions. The overall results exhibited the common pattern found in crowding tasks, namely, as target size and separation increased target size at threshold decreased. The fits were generally good and produced an average r^2 value of .93. As in Experiment 2a there seemed to be no effect of global stimulus configuration which is contrary to the results of Experiment 1 and somewhat surprising given the amount of literature that has found configuration can modulate the magnitude of crowding (e.g., Levi & Carney, 2009; Livne & Sagi, 2010; Poder & Wagemans, 2007; Saarela, 2010; Saarela, Sayim, Westheimer & Herzog, 2009).

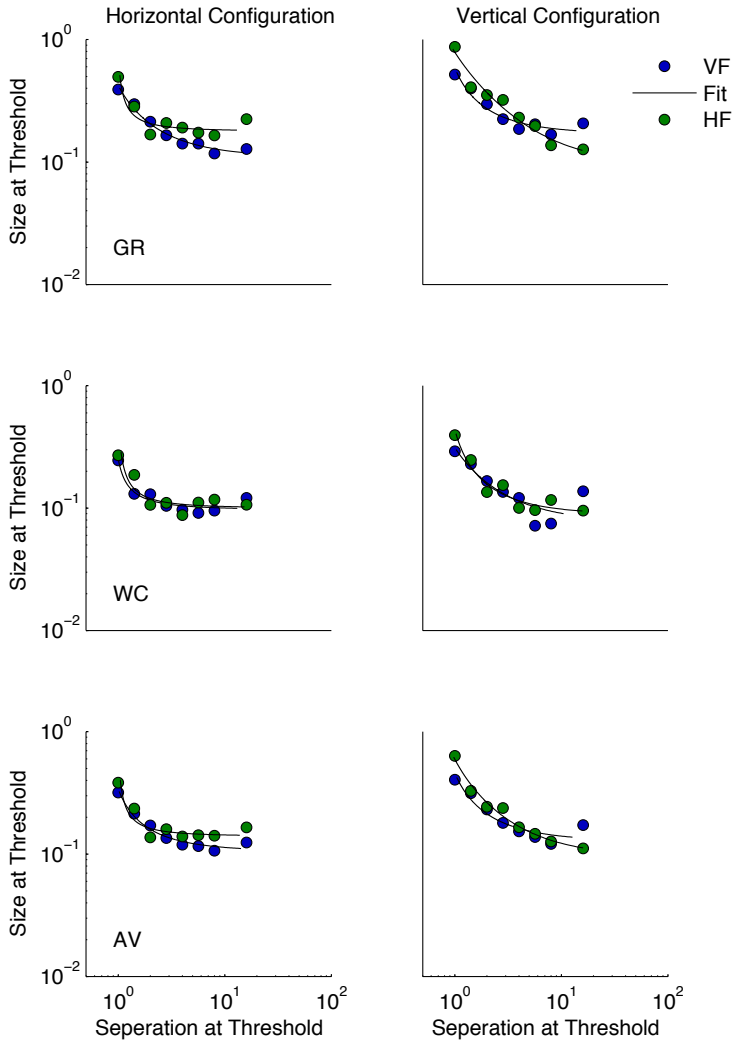

Figure 16. Experiment 2b: The Effect of Flanker Orientation. The effect of flanker orientation for two participants in the lower visual field on a log-log scale. Size-at-threshold is plotted along the y-axis and target-flanker separation is plotted on the x-axis. The three rows from top to bottom represent values for GR, WC and the averaged results. The left and right columns represent the horizontal and vertical configurations, respectively. Blue circles represent data points produced with vertical flankers and green circles depict horizontal flankers.

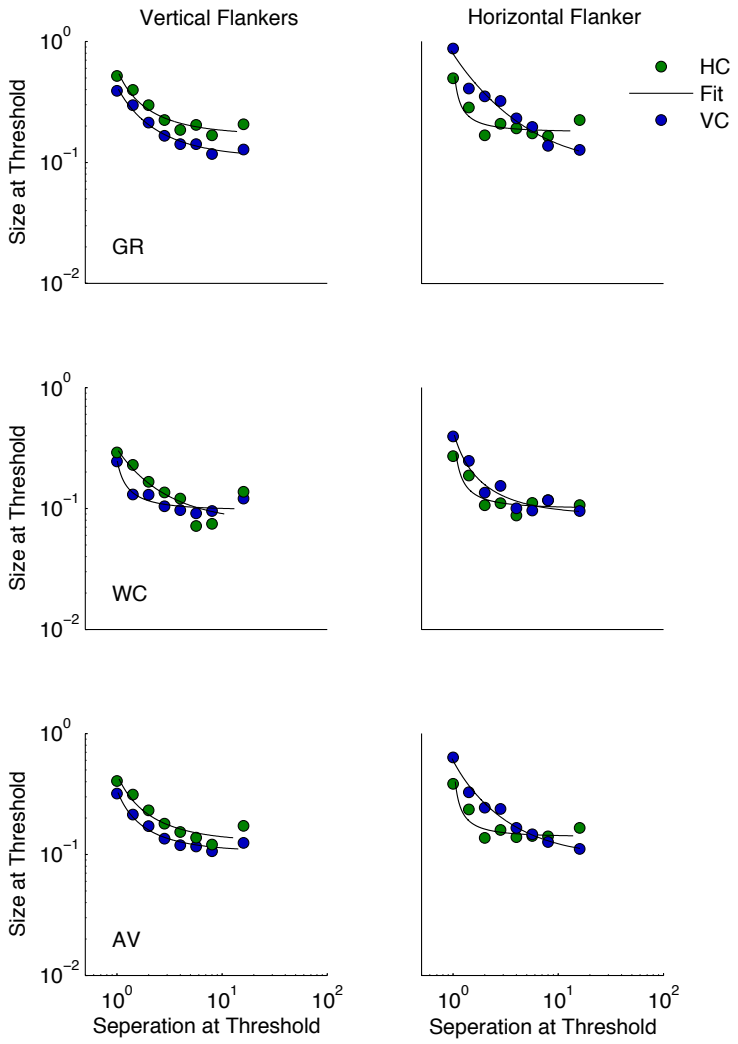

Figure 17. Experiment 2b: The Effect of Stimulus Configuration. The effect of configuration for two participants in the lower visual field plotted on a log-log scale. The designation of axes and rows are the same as in Figure 16. The left and right columns represent vertical and horizontal flankers respectively. Green circles represent data points produced in a horizontal configuration and blue circles represent those from a vertical configuration.

General Discussion

Bilateral mirror symmetry has often been thought of as a particularly salient stimulus property that is processed by specialized mechanisms tuned to its detection and discrimination in both humans and animals (e.g., Barlow & Reeves, 1979; Horridge, 1996; Locher & Wagemans, 1993; Swaddle, & Cuthill, 1993). Stimulus magnification has already been shown to compensate for eccentricity dependant sensitivity loss in the case of isolated symmetrical targets (Barrett al., 1999; Gurnsey et al., 1998a; Saarinen, 1988, Saarinen et al., 1989; Sally & Gurnsey, 2001; Tyler et al., 1995). However, stimuli are rarely presented to the visual system in isolation. The results of this set of experiments suggest that the visual system regards symmetry as simply another element to be processed within a crowded display. Using the method outlined by Gurnsey et al. (2011), Experiment 1 examined whether symmetry is subject to crowding effects. The study investigated issues similar to those often debated in the crowding literature: (a) the decrease or absence of the crowding effect at fixation, (b) increasing magnitude of spatial interference in the peripheral visual field and whether single or double linear magnification factors are required to characterize performance across the visual field, (c) and the presence of an anisotropy with respect to target-flanker configuration or visual field meridian.

The Five Fitting Methods of Experiment 1

As in most other studies of crowding that have used alternate stimuli or methods, we found target size-at-threshold for isolated (un-flanked) patches of symmetry increased linearly with eccentricity at a relatively modest rate. Conversely as target-flanker

separation increased target size-at-threshold began to decrease (Barrett et al., 1999; Gurnsey et al., 1998; Saarinen, 1988; Sally et al., 2001). At all eccentricities (Fig. 3) the ascending portion of the performance curves become almost parallel to the y-axis which suggests that at some point target size-at-threshold becomes entirely independent of target size. In other words, no matter the target size-at-threshold, target-flanker separation remains the same.

To fully characterize the data we attempted five fitting procedures described fully in the results section of Experiment 1. In all cases the fits were improved by the inclusion of eccentricity as a variable in the data (un-scaled data, Table 1, Expt. 1) and produced r^2 values of ≈ .96 across the analyses while the scaled data (Table 2, Expt. 1) produced fits of varying goodness and plausibility. The first two scaling methods were based on previous work by Poirier and Gurnsey (2002) and employed a double linear scaling procedure followed by a double scaling procedure requiring both a linear and nonlinear shift (r^2 = .71 and .65 respectively). These fits are moderate but they violate an essential assumption of crowding that the ratio of size (μ_{Size}) to separation (μ_{Size}) cannot be less than 1. Across both scaling procedures the ratio of target size-at-threshold to target-flanker separation fell in a range from .000029 to .59. See the results section for full details on the fitting procedures of 'Poirier and Gurnsey (2002): Double Linear Scaling Method' and 'Poirier and Gurnsey (2002): Linear/NonLinear Scaling Method' .

To answer to the implausibility of these predictions we attempted to fit the data using a method developed by Gurnsey et al. (2011) and modelled after the results of Latham and Whitaker (1996). The data were subjected to both a leftward and a downward shift that aligned the data on the x-axis with the point at which size-at-

threshold equals separation-at-threshold ($\mu_{Size} / \mu_{Sep} = 1$). Following, the data was fit using three methods, which produced the following r^2 values: .72, .55 and .63 (Table 2, Raw, LL and NLNL respectively). See the results section for full details on the three fitting procedures based on Gurnsey et al. (2011).

The 'Raw' scaling method based on Gurnsey et al. (2011) produced the best fit of the three and also produced tenable results that do not violate assumptions of the crowding phenomenon. In this study we found that $\bar{k}_V$ = .79 (SEM = .53) averaged over subjects and visual field. For simplicity we have chosen to represent our data with *k* to represent the rate of magnification ($E / E_2 = k * E$). Therefore smaller numbers represent slower rates of magnification (see Size Scaling in the Introduction for details).

Subject variability.

Previous reports have found individual $\bar{k}_V$ values that range from .49 to 1.62 (Barrett et al., 1999; Saarinen, 1988; Sally & Gurnsey, 2001). These are large differences from subject to subject and across studies when all participants were tested with a symmetrical stimulus. For all fits in the present study, with the exception of PG1 where the pattern was reversed, the scaled data for GR explained less variability then did the data for WC. One possibility for this variability is that the symmetrical patches were generated randomly on each trial. This prevented participants from performing the task through a template-matching strategy. Unfortunately it also means that two nominally identical stimuli (i.e., stimuli of identical size) might actually differ in 'perceptual salience' making it difficult to estimate thresholds reliably.

Crowding at fixation.

Although there was no evidence of crowding at fixation for the five largest target-flanker separations (2.32, 3.16, 4.31, 5.87, and 8.00) we did find modest interference effects at the smallest two separations (1.25, 1.70, Fig. 3). The threshold elevation ranged from 27 to 86% at fixation (0º). However, the smallest relative separation (1.25) translates to a centre-to-centre spacing of only .15° on average at fixation. It could be that the crowding effect at fovea is the result of internal blur given the complexity of our stimulus pattern (Levi, 2008). A consistent issue in the crowding literature is the near impossibility of making the stimuli at fixation (e.g., target and flankers) smaller than the internal blur while still being able to measure performance. As a result crowding and masking may get confused in the fovea so that what looks like crowding is actually partly masking (Levi et al., 2002a). It would be prudent to study crowding effects with simple line based symmetrical stimuli (i.e., mirrored 'S's) at a variety of sizes and line widths, up to 1º in all visual meridians to try and tease out the separate effects of blur, masking and crowding.

Can symmetry be double scaled?

Because the magnitude of the effect increased dramatically at 16º (elevation over the un-flanked threshold ranged from 243 to 697%, Fig. 3) we were unable to employ standard double linear magnification methods to shift all curves onto the foveal curve. As for other tasks, such as face- or subjective contour- perception (Melmoth et al., 2000; Poirier & Gurnsey, 2002), symmetry perception required multiple magnifications.

Figure 7 showed that the magnitude of crowding (green circles) increases with eccentricity at a faster rate than changes in un-flanked target size thresholds. The best-

fitting linear fits to these data give a mean $\bar{k}_H$ = 2.21 (SEM = .16). This is about 2.8 times greater than $\bar{k}_H$ = .79 and is consistent with previous studies employing different stimuli and tasks (Gurnsey et al., 2011; Latham & Whitaker, 1996; Toet & Levi, 2002). These results are consistent with studies in both the crowding and symmetry detection literature which suggest interference zones increase with eccentricity at a far greater rate than that of resolution thresholds (Barrett et al., 1999; Gurnsey et al., 1998a; Latham & Whitaker, 1996; Saarinen, 1988; Toet & Levi, 1992; Tyler et al., 1995).

In a recent study, Gurnsey et al. (2011) found that tasks may differ with respect to the relative rates at which the extent of interference zones and resolution limits change with eccentricity. The horizontal magnification factor (μ_E / μ_O) for the grating and T orientation discrimination tasks in the Gurnsey et al. study reach levels of 54 and 58, respectively, at 16° in the LowerVF, whereas for letter and symmetry discrimination (the present study) this ratio reaches only 33 and 38, respectively. The current study found $\bar{k}_V$ = .79 in the present symmetry task while Gurnsey et al. found .759 in the letter discrimination task and .54 and .57 in the grating and T orientation tasks, respectively. Therefore, the symmetry task studied here has more in common with the letter identification task than the grating and T orientation tasks. This is somewhat surprising as those tasks in Gurnsey et al. were orientation tasks similar to the one employed here, as opposed to discrimination of a specific letter. It is possible that symmetry and letter discrimination show greater sensitivity losses because of the inherent complexity of those stimuli as compared to a grating or letter ‘T’, regardless of the task at hand.

While we have not attempted to explore these differences further it could be that the complexity of the symmetrical stimuli may be more akin to the set of letters than the gratings or T figures used in the Gurnsey et al. (2011) paper. More clearly, orientation discrimination for simple figures is a relatively simple task therefore producing slower rates of eccentricity dependent sensitivity loss as compared to more demanding tasks (letter discrimination and orientation of symmetry discrimination) which produce faster rates of eccentricity dependent sensitivity loss.

The differences between the two studies suggest that it is important to further define the properties of symmetry. A symmetrical stimulus can be produced in a variety of ways. Historically, studies of symmetry detection and orientation discrimination at fixation have predominantly used random dot patterns or Gaussian blobs (e.g., Barlow & Reeves, 1979; Gurnsey et al., 1998a; Saarinen, 1988). In a study of orientation discrimination across the visual field Saarinen (1989) used simple line 'S's mirrored and rotated around the horizontal axis. Although there are similarities in the pattern of results produced with tasks using isolated symmetrical targets it is quite possible that symmetrical patterns of varying density will be affected differently by flanking stimuli and produce results quite different from the ones found here.

The shape of the interference zones.

Target size-at-threshold for both participants is highest when the flankers form a horizontal configuration around the target in the RightVF and when they are in the vertical configuration in the LowerVF (Expt. 1, Fig. 9). These results are in accord with the suggestion that the crowding regions are elliptical and oriented towards the fovea (Gurnsey et al., 2011; Pelli et al., 2007; Toet & Levi, 1992).

We saw no anisotropy with regard to visual field meridian at 0º however it is possible that one exists at 16º. On average, from the lower visual field to the right, the difference in percentage of threshold increase at 16º was 112.5% over the un-flanked threshold. However, participant GR showed a 625% increase as compared to 307% for participant WC, in the horizontal configuration in the right visual field, and a 345% increase as compared to 243% for the vertical configuration in the right visual field. It would be difficult to make any claims about visual field anisotropy with such discrepant values. We found no evidence of an anisotropy at 0º, as there was only a 7% difference between the lower and right visual fields. This result is contrary to previous work by He et al. (1996) who found a consistent crowding effect in an orientation discrimination task in the upper visual field as compared to the lower, from fixation to 20º eccentricity (an average difference of ≈ 26%).

The modest meridian effect is further complicated by the fact that for all five fitting methods (PG1, PG2, Raw, LL, NLNL; Tables 1 and 2) there was a large discrepancy in the amount of variability explained in the vertical configuration in the right visual field between the participants. For PG1, PG2, Raw, LL, and NLNL the difference between the r^2 values for the two participants was .42, .34, .20, .20 and .36, respectively.

Experiment 2a

The objective of Experiment 2a was to examine how the properties of the flankers themselves affect the degree of crowding (i.e., target size-at-threshold elevation). As in Experiment 1 (Fig. 2, 8º, purple circles) threshold values decreased as target-flanker spacing increased across conditions. Threshold elevation was the same for both parallel

and perpendicular flankers (Fig.14), and parallel and perpendicular configurations (Fig. 15). The lack of a configuration effect is contrary to a large literature (e.g., Exp. 1-Fig. 9; Pelli et al., 2007; Toet & Levi, 1992). Furthermore, the failure to find threshold elevation to be dependent on the relative orientations of the target and flankers is also inconsistent with the 90º orientation difference effects found by Levi & Carney (2009) and others. In other words, crowding was not noticeably alleviated by flankers rotated 90º from the target orientation.

The lack of effect for stimulus configuration bears further examination. Feng, Jiang and He (2007) used a variety of perceptual crowding tasks including orientation discrimination of a letter **T** when surrounded by four theta symbols and the gap in a Landolt **C**, to examine crowding effects. The stimuli were presented in the four quadrants of visual space at 7.6º eccentricity diagonal from fixation. In those conditions horizontal placement of the flankers created the greatest interference. However, in a control experiment, Feng et al. (2007) found that when stimulus trigrams were placed either horizontally along the horizontal meridian in line with fixation, or vertically along the vertical meridian in line with fixation, results were still in accord with the historical pattern based on the assumption that regions of interference are elliptical in shape and oriented towards the fovea (Pelli et al., 2007, Toet & Levi, 1992). The lack of effect in Experiments 2a and b seems to be an anomaly in the literature.

There was an effect of target orientation, vertical targets produced consistently lower thresholds than did horizontal ones, (Figs. 12 and 13). However, there was a great deal of participant variability in the data and the effect is seen consistently only for subject GR. This modest trend is consistent with a large literature that has found an

increased sensitivity to symmetrical targets with a vertical axis of orientation across the visual field (Barlow & Reeves, 1979; Jenkins, 1985)

It should be noted that Wenderoth (1994) found that the suggested hierarchy of orientation effects (perception is most accurate for a vertical axis of orientation, then horizontal, then diagonal [45 and 135º] followed by all other orientations) could be manipulated when observers were uncertain about the axis of orientation to be presented. In a series of experiments observers were asked to discriminate between a symmetrical target or random dot pattern presented at a number of orientations including and closely surrounding the vertical, horizontal and diagonal axes. The stimuli comprised 50 white dots presented on a black background subtending 20.5 degrees visual angle. When all orientations were presented with equal probability the axis hierarchy was consistent with previous literature (vertical, horizontal, diagonal [45 and 135º] then all others). But when the probability of another orientation rose, relative to the other orientations, the hierarchy followed suit and the highest percent correct was found for the most likely orientation to occur. The participants of the current study had to discriminate the orientation in a 2AFC task (with a 50% probability of vertical or horizontal orientation) and there was a still a clear effect of target orientation (Figs. 12 and 13). It makes sense to continue the examination of a vertical axis bias given the amount of literature devoted to the issue.

However, it might be useful to follow the example of Wenderoth (1994) and vary the likelihood of the vertical axis presentation. Perhaps, as in the study by Horridge (1996), which showed that the honeybee's preference for the vertically symmetrical signal was a learned behaviour rather than an innate bias, humans may be predisposed to

perceive vertical bilateral mirror symmetry given how often it is encountered by the visual system.

Experiment 2b

Experiment 2b used the Method of Constant Stimuli to hopefully eliminate some noisiness from the data that may have come about because of the Quest procedures' (Watson & Pelli, 1983) failure to converge on a threshold (see Subject Variability above). The experiment revisited the issue of stimulus configuration and flanker orientation and the data were noticeably cleaner with this method than in Experiment 2a for the same conditions.

The results replicated those of Experiment 2a, in that there was no effect of global stimulus configuration or target-flanker orientation contrast. This is somewhat surprising given the literature that has found such factors can modulate the magnitude of crowding (e.g., Levi & Carney, 2009; Livne & Sagi, 2010; Poder & Wagemans, 2007; Saarela, 2010; Saarela, Sayim, Westheimer & Herzog, 2009).

Future examinations of the type presented here may well benefit from the Method of Constant Stimuli, especially a re-examination of the target orientation effect found in Experiment 2a and the discrepant results regarding stimulus configuration in Experiments 1 and 2.

Conclusions

In sum, the results of the five analyses presented in Experiment 1 and the results of Experiments 2a and b suggest the following: (a) as for many other stimulus properties, crowding is modest or nonexistent at fixation (Figs. 2 and 3). (b) Regions of interference radiate outward from the fovea in an elliptical fashion (Fig. 9), (c) and the magnitude of

the crowding effect increases nonlinearly with eccentricity (Fig.7). Therefore, standard double linear scaling methods are not sufficient to collapse the data onto the foveal standard. In fact, standard double scaling methods predict implausible results, as at the smallest separations target and flanker would overlap and thus be considered masking rather than crowding. (d) Finally, sensitivity to a crowded symmetrical target drops off much faster with eccentricity than does resolution of an isolated symmetrical target consistent with other studies that have separated these two factors (Fig.7) (Latham & Whitaker, 1996; Gurnsey et al., 1998a). Taken together, these results suggest that symmetry is not particularly special to the early visual system. As for other stimuli symmetry discrimination degrades with decreasing separation between target and flanker and increasing eccentricity.

References

Bach, M. (1996). The Freiburg Visual Acuity test: Automatic measurement of visual acuity. *Optometry Visual Science*, 49-53. Retrieved from http://www.michaelbach.de/fract/index.html

Barlow, H. B. & Reeves, B. C. (1979) The versatility and absolute efficiency of detecting mirror symmetry in random dot displays. *Vision Research, 19*, 783-793. doi:10.1016/0042-6989(79)90154-8

Barrett, B. T., Whitaker, D., McGraw, P.V., & Herbert, A. M. (1999) Discriminating mirror symmetry in foveal and extra-foveal vision. *Vision Research*, *39*, 3737-3744. doi:10.1016/S0042-6989(99)00083-8

Bouma, H. (1970). Interaction effects in parafoveal letter recognition. *Nature, 226*(5241), 177-178.

Chung, S. T. L., Li, R. W., & Levi, D. M. (2007). Crowding between first and second order letter stimuli in normal foveal and peripheral vision. *Journal of Vision*, *7*, 1–13. doi:10.1167/7.2.10

Cowey, A. & Rolls, E.T. (1974) Human cortical magnification factor and its relation to visual acuity. *Experimental Brain Research, 21*, 447–454. Retrieved from http://www.ncbi.nlm.nih.gov/pubmed/4442497

Connolly, M. & Van Essen, D. (1984) The representation of the visual field in parvicellular and magnocellular layers of the lateral geniculate nucleus in the macaque monkey. *Journal of Comparative Neurology*, *226*(4), 544-64. Retrieved from http://www.ncbi.nlm.nih.gov/pubmed/6747034.

Danilova, M. V. & Bondarko, V. M. (2007). Foveal contour interactions and crowding effects at the resolution limit of the visual system. *Journal of Vision, 7*(2):25, 21-18. doi: 10.1167/7.2.25

Daniel, P. M. & Whitteridge, D. (1961) The representation of the visual field on the cerebral cortex of monkeys. *Journal of Physiology, 159*, 203-221. Retrieved from http://jp.physoc.org/content/159/2/203.long

Drasdo, N. (1977) The neural representation of visual space. *Nature*, *266*(5602), 554-556. Retrieved from http://www.ncbi.nlm.nih.gov/pubmed/859622.

Dow, B. M., Snyder, A.Z., Vautin, R. G., & Bauer, R. (1981) Magnification factor and receptive field size in foveal striate cortex of the monkey. *Experimental Brain Research*, *44*(2):213-28. doi: 10.1007/BF00237343

Feng, C., Jiang, Y. & He, S. (2007). Horizontal and vertical asymmetry in visual spatial crowding effects. *Journal of Vision, 7*(2):13, 1-10. doi: 10.1167/7.2.13

Flom, M. C., Weymouth, F. W., & Kahneman, D. (1963) Visual resolution and contour interaction. *Journal of the Optical Society of America, 53*(9), 1026-1032. Retrieved from http://www.ncbi.nlm.nih.gov/pubmed/14065335

Gurnsey, R., Herbert, A. M., & Kenemy, J. (1998a). Bilateral symmetry embedded in noise is detected accurately only at fixation. *Vision Research*, *38*, 3795-3803. doi:10.1016/S0042-6989(98)00106-0

Gurnsey, R., Herbert, A., & Nguyen-Tri, D. (1998b). Bilateral Symmetry is not detected in parallel. Canadian Society for Brain, Behaviour and Cognitive Science. June, Ottawa.

Gurnsey, R., Roddy, G., & Chanab, W. (2011). Crowding and multiple magnification theory. *Journal of Vision*, *11*(7), [in process] doi: 10.1167/11.7.15

Gurnsey, R., Roddy, G., Ouhnana, M., & Troje, N. F. (2008) Stimulus magnification equates identification and discrimination of biological motion across the visual field. *Vision Research, 48*(28), 2827-2834. doi:10.1016/j.visres.2008.09.016

He, S., Cavanagh, P., & Intriligator, J. (1996) Attentional resolution and the locus of visual awareness. *Nature, 383*(6598), 334-337. doi:10.1016/S1364-6613(97)89058-4

Hodgson, D. (2011) The first appearance of symmetry in the human lineage: Where perception meets art. *Symmetry*, *3*, 37-53. doi:10.3390/sym3010037

Horridge, G. A. (1996). The honeybee (*Apis mellifera*) detects bilateral symmetry and discriminates its axis, *Journal of Insect Physiology.* 42, 755–764. Retrieved from http://www.mendeley.com/research/the-honeybee-apis-mellifera-detects-bilateral-symmetry-and-discriminates-its-axis-1/

Hubel, D. H. & Weisel, T. N. (1974) Uniformity of monkey striate cortex: a parallel relationship between field size, scatter, and magnification factor. *Journal of Comparative Neurology*, *158*(3), 295-305. doi: 10.1002/cne.901580305

Jenkins, B. (1982) Redundancy in the perception of bilateral symmetry in dot textures. *Perception & Psychophysics, 32*(2), 171 – 177. doi: 10.3758/BF03204276

Jenkins, B. (1983) Component processes in the perception of bilaterally symmetric dot textures. *Perception & Psychophysics, 34*, 433-440. doi: 10.3758/BF03203058

Jenkins, B. (1985) Orientational Anistropy in the human visual system. *Perception & Psychophysics, 37*(2), 125-134. doi: 10.3758/BF03202846

Kleiner M, Brainard, D. H., & Pelli, D. G. (2007). What's new in Psychtoolbox-3? *Perception (ECVP Abstract Supplement)*, 14.

Korte, W. (1923) Uber die Gestaltauffassung im indirekten Sehen. Zeitschrift fu¨r Psychologie, 93, 17–82, Quoted translation by Uta Wolfe appeared in Pelli et al. 2004.

Latham, K. & Whitaker, D. (1996) Relative roles of resolution and spatial interference in foveal and peripheral vision. *Ophthalmic Physiological Optics*, *61* (1), 49-57. doi: 10.1046/j.1475-1313.1996.95001247.x

Levi, D. M. (2008) Crowding-an essential bottleneck for object recognition: a mini-review. *Vision Research, 48*(5), 635-654. doi:10.1016/j.visres.2007.12.009

Levi, D. M. & Carney, T. (2009) Crowding in peripheral vision: Why bigger is better. *Current Biology, 19*, 1988-1993. doi: 10.1167/11.1.10

Levi, D. M., Hariharan, S., & Klein, S. A. (2002a) Suppressive and facilitatory spatial interactions in peripheral vision: peripheral crowding is neither size invariant nor simple contrast masking. *Journal of Vision, 2*(2), 167-177. doi:10.1167/2.2.3

Levi, D. M., Klein, S. A., & Aitsebaomo, A.P., (1985) Vernier acuity, crowding and cortical magnification. *Vision Research, 25,* 963-977. doi:10.1016/0042-6989(85)90207-X

Levi, D. M., Klein, S. A., & Hariharan, S. (2002b) Suppressive and facilitatory spatial interactions in foveal vision: foveal crowding is simple contrast masking. *Journal of Vision, 2*(2), 140-166. doi:10.1167/2.2.2

Liu, L., & Arditi, A. (2000) Apparent string shortening concomitant with letter crowding. *Vision Research, 40,* 1059-1067. doi:10.1016/S0042-6989(99)00247-3

Livne, T. & Sagi, D. (2010) How do flankers relations affect crowding? *Journal of Vision*, *10*(3), 1-14. doi:10.1167/10.3.1

Locher, P. J. & Wagemans, J. (1993) Effects of element type and spatial grouping on symmtery detection. *Perception*, *22*(5), 565-587. doi:10.1068/p220565

Makela, P., Whitaker, D., & Rovamo, J. (1993). Modelling of orientation discrimination across the visual field. *Vision Research*, *33*, 723–730. doi:10.1016/0042-6989(93)90192-Y

Melmoth, D. R., Kukkonen, H. T., Mäkelä, P. K., & Rovamo, J. M. (2000). The effect of contrast and size scaling on face perception in foveal and extrafoveal vision. *Investigative Ophthalmology and Visual Science, 41*(9), 2811-2819. Retrieved from http://www.iovs.org/content/41/9/2811.full.pdf+html

Moriyama, M. & Moriyama, M. (1999) A comparison between asymmetric Japanese Ikebana and symmetric western flower arrangement. *Forma*, *14*, 355-361. Retrieved from http://beepdf.com/doc/77592/a_comparison_between_asymmetric_japanese_ikebana_and_symmetric_western_.html

Olivers, C. N. L. & Peter van der Helm (1998) Symmetry and selective attention: A dissociation between effortless perception and serial search. *Perception and Psychophysics, 60*(7), 1101-1116. doi: 10.3758/BF03206161

Parkes, L., Lund, J., Angelucci, A., Solomon, J. A., & Morgan, M. (2001). Compulsory averaging of crowded orientation signals in human vision. *Nature Neuroscience, 4,* 739-744. doi:10.1038/89532

Pelli, D. G. (2008). Crowding: a cortical constraint on object recognition. *Current Opinion in Neurobiology, 18*(4), 445-451. doi: 10.1016/j.conb.2008.09.008

Pelli, D. G., Palomaras, M., & Majaj, N. J. (2004). Crowding is unlike ordinary masking: Distinguishing feature integration from detection. *Journal of Vision*, *4*, 1136-1169. doi:10.1167/4.12.12

Pelli, D. G., Tillman, K. A., Freeman, J., Su, M., Berger, T. D., & Majaj, N. J. (2007). Crowding and eccentricity determine reading rate. *Journal of Vision, 7*(2), 21-36. doi:10.1167/7.2.20

Perry, H. V. & Cowey, A. (1985) The ganglion cell and cone distributions in the monkey's retina: Implications for central magnification factors. *Vision Research*, *25*(12), 1795-1810. doi:10.1016/0042-6989(85)90004-5

Petrov, Y. & Popple, A. V. (2007) Crowding and surround suppression: Not to be confused. *Journal of Vision*, *7*(2), 1–9. doi: 10.1167/7.2.12

Poder, E. (2008) Crowding with coarse detection and coarse discrimination of simple visual features. *Journal of Vision*, *8*(4):24, 1-6. doi: 10.1167/8.4.24

Poder, E., & Wagemans, J. (2007) Crowding with conjunctions of simple features. *Journal of Vision*, *7*(2):23, 1-12. doi: 10.1167/7.2.23

Poirier, F. J. A. M. & Gurnsey, R., (1998). The effects of eccentricity and spatial frequency on the orientation discrimination asymmetry. *Spatial Vision*, 349-66. doi: 10.1163/156856898X00077

Poirier, F. J. A. M., & Gurnsey, R. (2002). Two eccentricity-dependent limitations on subjective contour discrimination. *Vision Research, 42*(2), 227-238. doi:10.1016/S0042-6989(01)00273-5

Rovamo, J., & Virsu, V. (1979). An estimation and application of the human cortical magnification factor. *Experimental Brain Research, 37*(3), 495-510. doi: 10.1007/BF00236819

Saarela, T. P., Sayim, B., Westheimer, G., & Herzog, M. H. (2009). Global stimulus configuration modulates crowding. *Journal of Vision*, *9*(2):5, 1–11. doi:10.1167/9.2.5

Saarela, T. P., Westheimer, G., & Herzog, M. H. (2010). The effect of spacing regularity on visual crowding. *Journal of Vision*, *10*(10):17, 1–7. doi:10.1167/10.10.17

Saarinen, J. (1988) Detection of mirror symmetry in random dot patterns at different eccentricities. *Vision Research*, *28* (6), 755-759. doi:10.1016/0042-6989(88)90054-5

Saarinen, J, Rovamo, J., & Virsu, V. (1989). Analysis of spatial structure in eccentric vision. *Investigative Ophthalmology and Vision Science*, *30* (2), 293-296. Retrieved from http://www.iovs.org/content/30/2/293.long

Sally, S., & Gurnsey, R. (2001). Symmetry detection across the visual field. *Spatial Vision*, *14*(2), 217-234. doi: 10.1163/156856801300202940

Strasburger, H., Harvey, L. O., Jr., & Rentschler, I. (1991). Contrast thresholds for identification of numeric characters in direct and eccentric view. *Perception and Psychophysics, 49,* 495-508. Retrieved from

http://www.mendeley.com/research/contrast-thresholds-identification-numeric-characters-direct-eccentric-view/

Swaddle, J. P., & Cuthill, I. C. (1993) Preference for symmetric males by female zebra finches. *Nature*, *367*, 165-166. doi:10.1038/367165a0

Thibos, L. N., Still, D. L., & Bradley, A. (1996) Characterization of spatial aliasing and contrast sensitivity in peripheral vision. *Vision Research, 36*(2), 249-258. doi:10.1016/0042-6989(95)00109-D

Thibos, L. N., Cheney, F. E., & Walsh, D. J. (1987) Retinal limits to the detection and resolution of gratings. *Journal of the Optical Society of America, 4*(8), 1524-1529. doi:10.1364/JOSAA.4.001524

Toet, A., & Levi, D. M. (1992). The two-dimensional shape of spatial interaction zones in the parafovea. *Vision Research, 32*(7), 1349-1357. **doi:** 10.1163/156856894X00350

Treisman, A. M. & Gelade, G. A (1980) Feature-integration theory of attention. *Cognitive Psychology, 12*, 97-136, doi:0010-0285(80)90005-5

Tripathy, S. P. & Cavanagh, P. (2002) The extent of crowding in peripheral vision does not scale with target size, *Vision Research*, *42*, 2357-2369. doi:10.1016/S0042-6989(02)00197-9

Tyler, C. W. & Hardage, L. (1996) In Tyler, C. W., Editor. Human Symmetry Perception, Utrecht, Netherlands: VSP, 157-171.

Tyler, C. W., Hardage, L., & Miller, R. T. (1995) Multiple mechanisms for the detection of mirror symmetry. *Spatial Vision*, *9* (1), 79-100. doi: 10.1163/156856895X00124

Van der Helm, P. (2011) The influence of perception on the distribution of multiple symmetries in nature and art. *Symmetry*, *3*, 51-71. doi:10.3390/sym3010054

Virsu, V., Näsänen, R., & Osomoviita, K. (1987) Cortical magnification and peripheral vision. *Journal of the Optical Society of America, 4*(8), 1568-1578. doi:10.1364/JOSAA.4.001568

Wagemans, J. (1992) Perceptual use of nonaccidental properties. *Canadian Journal of Psychology, 46,* 236-279. doi: 10.1037/h0084323

Wagemans, J. (1993) Skewed symmetry: A nonaccidental property used to perceive visual forms. *Journal of Experimental Psychology: Human Perception and Performance*, *19*, 364-380. Retrieved from http://www.sciencedirect.com/science/article/pii/S0096152302009379

Wagemans, J. (1995) Detection of visual symmetries. *Spatial Vision*, *9*, 9-32. Retrived from *www.ncbi.nlm.nih.gov/pubmed/7626549*

Watson, A. B. (1987) Estimation of local spatial scale. *Journal of the Optical Society of America A*, *4*, 1579–1582. doi:10.1364/JOSAA.4.001579

Watson, A. B., & Pelli, D. G. (1983). QUEST: A Bayesian adaptive psychometric method. *Perception & Psychophysics*, *33*, 113-120. Retrieved from http://academic.research.microsoft.com/Publication/1972926

Wenderoth, P. (1994) The salience of vertical symmetry. *Perception*, *23*, 221-236. Retrieved from http://www.perceptionweb.com/abstract.cgi?id=p230221

Westheimer, G. (1982) The spatial grain of the perifoveal visual field. *Vision Research*, *22*(1), 157-162. doi:10.1016/0042-6989(82)90177-8

Weymouth, F. W. (1958) Visual sensory units and the minimal angle of resolution. *American Journal of Ophthalmology, 46*, 102-113.

Whitaker, D., Rovamo, J., MacVeigh, D., & Mäkelä, P. (1992) Spatial scaling of vernier acuity tasks. *Vision Research, 32*(8), 1481-1491. doi:10.1016/0042-6989(92)90204-V

Whitney, D., & Levi, D. (2011) Visual crowding: a fundamental limit on conscious perception and object recognition. *Trends in Cognitive Sciences*, *15*(4), 160-168. doi:10.1016/j.tics.2011.02.005

Wilson, H. R., Levi, D., Maffei, L., Rovamo, J., & DeValois, R. (1990) The perception of form: Retina to striate cortex. In L. Spillman and J. S. Werner (Eds.), Visual Perception, The Neurophysiological Foundations. (pp. 231-272). Academic Press, Inc.

Table 1

Proportion of explained variability (r^2) including eccentricity as a variable (un-scaled data) for each fitting method in Experiment 1

Method	PG1		PG2		Raw		LL		NLNL	
Participant	GR	WC	GR	WC	GR	WC	GR	WC	GR	WC
H-RVF	0.97	0.95	0.97	0.98	0.93	0.99	0.97	0.96	0.96	0.98
H-LVF	0.98	0.98	0.98	0.98	0.99	0.99	0.98	0.98	0.98	0.98
V-RVF	0.93	0.95	0.72	0.97	0.98	0.99	0.92	0.96	0.95	0.97
V-LVF	0.90	0.97	0.98	0.82	0.99	0.99	0.98	0.98	0.99	0.98
Mean*	0.95	0.96	0.91	0.94	0.97	0.99	0.96	0.97	0.97	0.98
Mean+	0.95		0.93		0.98		0.97		0.97	

Note. PG1 and PG2 = Poirier & Gurnsey (2002): Double Scaling Method and :Linear/Nonlinear Scaling Method respectively.
GR and WC are the two participants.
Raw, LL and NLNL = Gurnsey et al., 2011: 'Raw' Scaling Method, :Two Linear Scaling Factors and :Two Nonlinear Scaling Factors respectively.
H-RVF and H-LVF = Horizontal Configuration-Right Visual Field and Lower Visual Field respectively.
V-RVF and V-LVF = Vertical Configuration-Right Visual Field and Lower Visual Field respectively.
* Mean calculated for each participant across conditions for each fitting procedure.
+ Mean calculated across participants and across conditions for each fit fitting procedure.

Table 2

Proportion of explained variability (r^2) in the scaled data for each fitting method in Experiment 1

Method	PG1		PG2		Raw		LL		NLNL	
Participant	GR	WC	GR	WC	GR	WC	GR	WC	GR	WC
HRVF	0.61	0.43	0.62	0.66	0.59	0.67	0.61	0.43	0.62	0.66
HLVF	0.99	0.99	0.93	0.94	0.78	0.84	0.99	0.99	0.93	0.94
VRVF	0.98	0.56	0.34	0.68	0.63	0.83	0.98	0.56	0.34	0.68
VLVF	0.53	0.56	0.58	0.48	0.71	0.71	0.53	0.56	0.58	0.48
Mean*	0.78	0.64	0.62	0.69	0.68	0.76	0.78	0.64	0.62	0.69
Mean+	0.71		0.65		0.72		0.55		0.63	

Refer to Table 1 notes for identification of column and row headings.
* Mean calculated for each participant across conditions for each fitting procedure.
+ Mean calculated across participants and across conditions for each fit fitting procedure.

Table 3

The eight stimulus sizes used in Experiment 2b at each of the 7 relative separations (and ∞ - the un-flanked condition)

Relative Separation (x Target Size)							
∞ *	8.00	5.66	4.00	2.83	2.00	1.41	1.00
2.52	2.52	2.52	2.52	3.02	3.63	4.35	5.22
1.84	1.84	1.84	1.84	2.21	2.65	3.18	3.82
1.34	1.34	1.34	1.34	1.62	1.94	2.32	2.79
0.98	0.98	0.98	0.98	1.18	1.41	1.70	2.04
0.72	0.72	0.72	0.72	0.86	1.04	1.24	1.49
0.53	0.53	0.53	0.53	0.63	0.76	0.90	1.09
0.39	0.39	0.39	0.39	0.46	0.55	0.67	0.80
0.28	0.28	0.28	0.28	0.34	0.41	0.48	0.58

Note. Column headings refer to Relative Separation.
Sizes are reported in each column as Relative Separation * Target Size
* Infinity or the un-flanked condition.